PROPAGATION OF MULTIWAVELENGTH LASER RADIATION THROUGH ATMOSPHERIC TURBULENCE

J. Richard Kerr, et al

Oregon Graduate Center

Prepared for:

Rome Air Development Center
Defense Advanced Research Projects Agency

July 1975

RADC-TR-75-181
Technical Report
July 1975

PROPAGATION OF MULTIWAVELENGTH LASER RADIATION THROUGH ATMOSPHERIC TURBULENCE

Oregon Graduate Center

Sponsored by
Defense Advanced Research Projects Agency
ARPA Order No. 1279

Approved for public release;
distribution unlimited.

The views and conclusions contained in this document are those of the authors and should not be interpreted as necessarily representing the official policies, either expressed or implied, of the Defense Advanced Research Projects Agency or the U. S. Government.

Rome Air Development Center
Air Force Systems Command
Griffiss Air Force Base, New York 13441

This report has been reviewed by the RADC Information Office (OI) and is releasable to the National Technical Information Service (NTIS). At NTIS it will be releasable to the general public including foreign nations.

This report has been reviewed and is approved for publication.

APPROVED: Darryl P. Greenwood

DARRYL P. GREENWOOD, Capt, USAF
Project Engineer

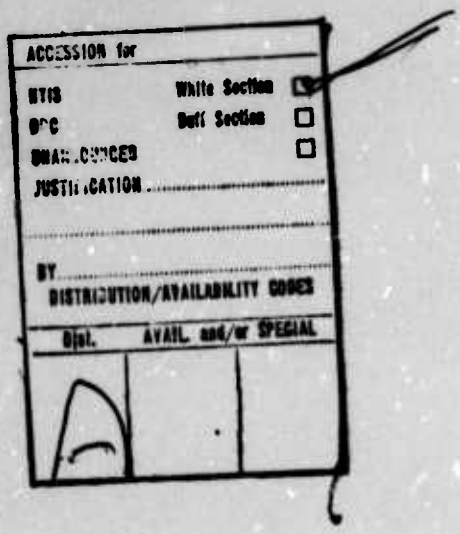

Do not return this copy. Retain or destroy.

UNCLASSIFIED

SECURITY CLASSIFICATION OF THIS PAGE (When Data Entered)

REPORT DOCUMENTATION PAGE		READ INSTRUCTIONS BEFORE COMPLETING FORM
1. REPORT NUMBER RADC-TR-75-181	2. GOVT ACCESSION NO.	3. RECIPIENT'S CATALOG NUMBER
4. TITLE (and Subtitle) PROPAGATION OF MULTIWAVELENGTH LASER RADIATION THROUGH ATMOSPHERIC TURBULENCE		5. TYPE OF REPORT & PERIOD COVERED Interim Technical Report 1 Sep 74 - 31 Mar 75
		6. PERFORMING ORG. REPORT NUMBER N/A
7. AUTHOR(s) J. Richard Kerr, Richard A. Elliott James R. Dunphy, Philip A. Pincus		8. CONTRACT OR GRANT NUMBER(s) F30602-74-C-0082
9. PERFORMING ORGANIZATION NAME AND ADDRESS Oregon Graduate Center 19600 N. W. Walker Road Beaverton OR 97005		10. PROGRAM ELEMENT, PROJECT, TASK AREA & WORK UNIT NUMBERS 62301E 12790212
11. CONTROLLING OFFICE NAME AND ADDRESS Defense Advanced Research Projects Agency 1400 Wilson Boulevard Arlington VA 22209		12. REPORT DATE July 1975 13. NUMBER OF PAGES 49
14. MONITORING AGENCY NAME & ADDRESS (if different from Controlling Office) Rome Air Development Center (OCSE) Griffiss AFB NY 13441		15. SECURITY CLASS. (of this report) UNCLASSIFIED 15a. DECLASSIFICATION DOWNGRADING SCHEDULE N/A

16. DISTRIBUTION STATEMENT (of this Report)

Approved for public release; distribution unlimited.

17. DISTRIBUTION STATEMENT (of the abstract entered in Block 20, if different from Report)

Same

18. SUPPLEMENTARY NOTES

RADC Project Engineer:
Capt. Darryl P. Greenwood (OCSE)

19. KEY WORDS (Continue on reverse side if necessary and identify by block number)

Propagation
Turbulence
Atmospheric Optics
Scintillation

20. ABSTRACT (Continue on reverse side if necessary and identify by block number)

Recent work on the short-term statistics of scintillation is extended to a more detailed investigation of the effective number of independent turbulence regions on a propagation path as a function of wind direction and other parameters. The resultant effect on the spread in strength-of-fluctuation measurements vs. averaging time is discussed, including both microthermal and scintillation data and their interrelationship. These considerations are related to spatial correlation measurements of the turbulence strength (microthermal envelope) as

DD FORM 1 JAN 73 1473 EDITION OF 1 NOV 65 IS OBSOLETE

UNCLASSIFIED

SECURITY CLASSIFICATION OF THIS PAGE (When Data Entered)

a function of averaging time, including the influence of pronounced intermittency of turbulence.

In a related discussion, the conditional statistics of scintillation, based on an initial comparison of the instantaneous target irradiance with a predetermined threshold level, are investigated as a function of elapsed time. With the assumption that the two-point log scintillation process is a bivariate normal, the problem is readily solvable using empirically derived correlation functions. The validity and limitations of this assumption are briefly considered, and representative results are given.

New multiwavelength facilities are described which will be used for the completion of the experiments on mean target irradiance and its fluctuations, with and without cancellation of turbulence-induced beam wander. Other near-term plans are also briefly reviewed.

PROPAGATION OF MULTIWAVELENGTH LASER RADIATION THROUGH ATMOSPHERIC TURBULENCE

J. Richard Kerr
James R. Dunphy
Richard A. Elliott
Philip A. Pincus

Contractor: Oregon Graduate Center
Contract Number: F30602-74-C-0082
Effective Date of Contract: 1 December 1973
Contract Expiration Date: 31 July 1975
Amount of Contract: $129,699.00
Program Code Number: 4E20
Period of work covered: 1 Sep 74 - 31 Mar 75

Principal Investigator: Dr. J. Richard Kerr
Phone: 503 645-1121

Project Engineer: Capt Darryl P. Greenwood
Phone: 315 330-3145

This research was supported by the Defense Advanced Research Projects Agency of the Department of Defense and was monitored by Capt Darryl P. Greenwood, RADC (OCSE), Griffiss AFB NY 13441.

Summary

Recent work on the short-term statistics of scintillation is extended to a more detailed investigation of the effective number of independent turbulence regions on a propagation path as a function of wind direction and other parameters. The resultant effect on the spread in strength-of-fluctuation measurements vs. averaging time is discussed, including both microthermal and scintillation data and their interrelationship. These considerations are related to spatial correlation measurements of the turbulence strength (microthermal envelope) as a function of averaging time, including the influence of pronounced intermittency of turbulence.

In a related discussion, the conditional statistics of scintillation, based on an initial comparison of the instantaneous target irradiance with a predetermined threshold level, are investigated as a function of elapsed time. With the assumption that the two-point log scintillation process is a bivariate normal, the problem is readily solvable using empirically derived correlation functions. The validity and limitations of this assumption are briefly considered, and representative results are given.

New multiwavelength facilities are described which will be used for the completion of the experiments on mean target irradiance and its fluctuations, with and without cancellation of turbulence-induced beam wander. Other near-term plans are also briefly reviewed.

TABLE OF CONTENTS

I. INTRODUCTION

This report will briefly summarize recent progress and ongoing efforts on several topics in optical propagation through atmospheric turbulence. In Section II, we describe some further results on the short-term statistics of turbulence and scintillation, which supplements the detailed treatment given in the preceding report on this program. In Section III, we discuss a new topic, the conditional fading statistics of a scintillating signal or target illumination, in which the state of the "channel" is investigated immediately following the onset of a "good" interval. Finally, in Section IV we describe new experimental work and facilities, including multiwavelength target-irradiance investigations with beam-wander cancellation, very-long-path or strong-scattering scintillation phenomena, and other areas of interest.

II. FURTHER RESULTS ON SHORT-TERM STATISTICS

In the preceding technical report on this program,[1] we presented a complete theoretical treatment of the short-term statistics of turbulence and scintillation, including data-spread and confidence-interval considerations as a function of averaging time. In this section, we supplement the previous discussion with representative results of recent experiments on this topic. Our related work on computer simulation of the short-term propagation problem will be described in a subsequent report.

A. Relationship Between Microthermal and Scintillation Data Spread

In a discretized model of the propagation path,[1] we idealize the turbulence into N elements, the strength of turbulence being totally correlated throughout one element and totally uncorrelated between any two elements. The length of an element depends on the averaging time

---

1. J. R. Kerr, et al, "Propagation of Multiwavelength Laser Radiation Through Atmospheric Turbulence," RADC-TR-74-320, November, 1974.

(τ) used in determining "strength of turbulence" $\left(C_{n_\tau}^2\right)$, and on the direction of the wind relative to the path. The variance of a set of measurements of the scintillation log amplitude variance $\left(\text{Var } \sigma_\tau^2\right)$ is then related to the variance of microthermal measurements $\left(\text{Var } C_{n_\tau}^2\right)$ by

$$\frac{\text{Var } \sigma_\tau^2}{\overline{\sigma^2}^2} = \frac{\text{Var } C_{n_\tau}^2}{\overline{C_n^2}^2} \cdot \frac{1}{N_{eff}} \quad . \tag{1}$$

The quantity $N_{effective}$ is derived from N, the number of correlation lengths of $C_{n_\tau}^2$ along the path, and the spatial weighting function (f) determined by beam geometry. If the log amplitude variance is written as

$$\sigma^2 = \sum_{i=1}^{N} f_i \, C_{n_i}^2 \tag{2}$$

then we have

$$N_{eff} = \frac{\left(\sum_{i=1}^{N} f_i\right)^2}{\sum_{i=1}^{N} f_i'^2} \leq N \tag{3}$$

For a spherical wave, f is a discrete approximation to

$$f(z) \sim \left(\frac{z}{L}\right)^{5/6} (L-z)^{5/6} \quad , \tag{4}$$

where z is the path variable and L is the total pathlength. In the case of e.g. focused beams or other systems yielding more localized weighting functions, N_{eff} becomes much less than N and Var σ_τ^2 increases accordingly. In the limit of f as a delta function, the variance in σ_τ^2 for any given τ will be the same as that for $C_{n_\tau}^2$.

For averaging times greater than the integral scale of the squared microthermal fluctuations ($I_{\Delta T^2}$), the normalized variance of $C_{n_\tau}^2$ measurements will be inversely proportional to τ (Ref. 1). The corresponding dependence for the normalized variance of σ_τ^2 depends on the wind field. If we extend our idealization to assume large-scale regular flow with "frozen-in" strength of turbulence over scales comparable with the pathlength, we may distinguish the following two cases:

1. When the wind is parallel to the path, the z-correlation length of $C_{n_\tau}^2$ is proportional to τ, which cancels the usual effect of increased averaging, and thus Var σ_τ^2 is independent of τ. That is, $N \sim \tau^{-1}$, to be consistent with Eq. 1.
2. When the wind is perpendicular to the path, the z-correlation length is independent of τ, Var $\sigma_\tau^2 \sim \tau^{-1}$, and N is independent of τ.

When we compare this useful but idealized conceptual model to experimental data, subtleties and complications immediately arise, as shown by the following examples. In Table I, we show the basic parameters of nine experimental runs comparing normalized C_n^2 and σ^2 variances vs. averaging time. Runs 1-6 involve winds basically parallel to the path, and the results for $1/N_{eff}$ (Eq. 1) are shown in Fig. 1a. According to the foregoing reasoning, we would ideally expect a slope of +1 for these curves, and a tendency to break in this direction may be noted. In Fig. 1b, curves are given for wind directions partially or entirely perpendicular to the path; two of these tend to be flat, as expected. Taking into account all conditions and averaging times, values of N_{eff} were seen to range from approximately 8 to 200.

TABLE I

Parameters for Data on Var $C_{n_{\bar{\tau}}}^2$ and Var σ_τ^2 Shown in Figs. 1, 2,

Run No.	Symbol on Figs.	v(m/sec)	Wind Direction Relative to Optical Path	$\bar{\sigma}^2$
1	○	3.5	0°	0.31
2	□	<1	0°	0.24
3	◇	3	0°	0.28
4	△	3.5	180°	0.30
5	+	9	-15°	0.076
6	✱	3.5	195°	0.31
7	•	4	-45°	0.25
8	▲	0.5-2	90°	0.33
9	■	1.5	90°	0.32

Wavelength: 4880Å

Pathlength: 1.6 km

Beam Geometry: Approximate Spherical Wave

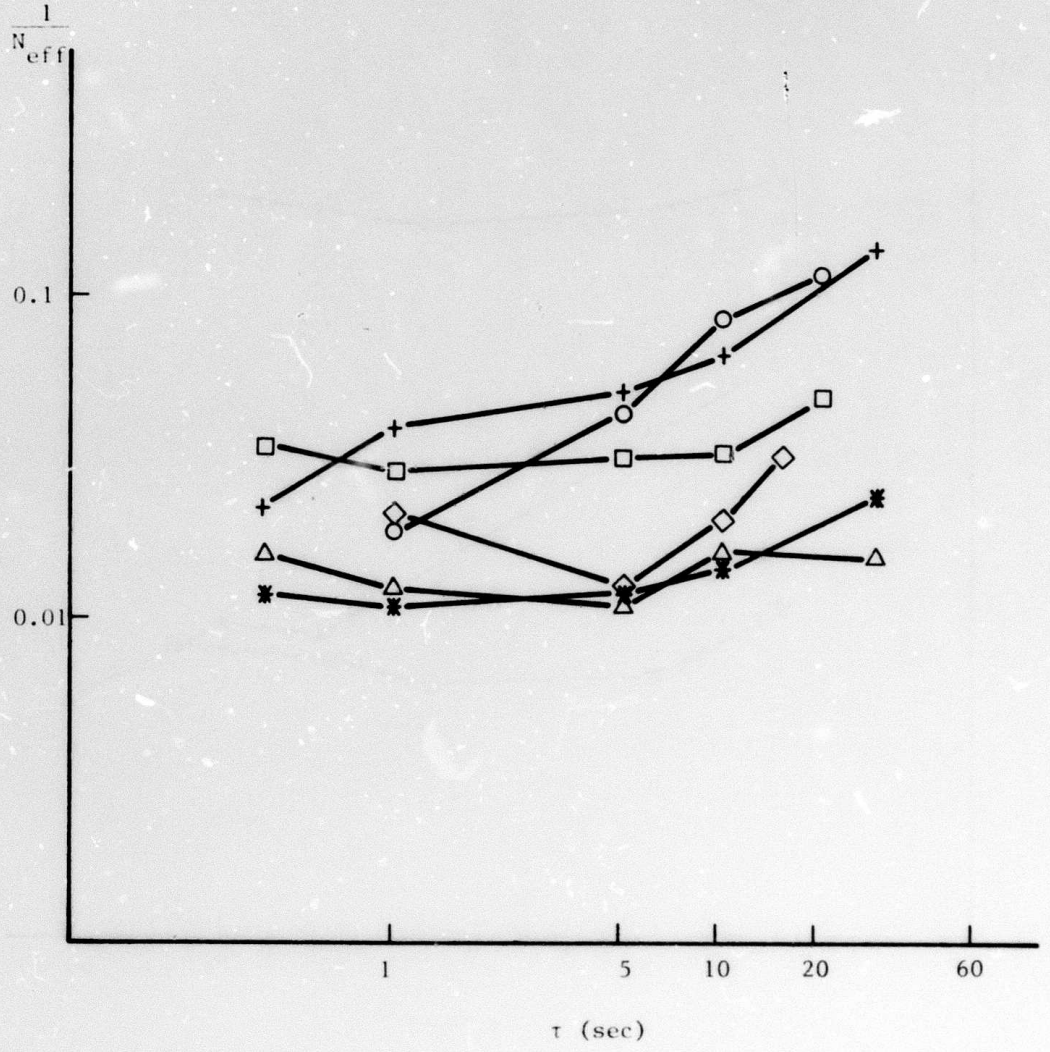

Figure 1a. The reciprocal number of effectively-independent turbulence regions $\left(\frac{1}{N_{eff}}\right)$ along a propagation path, vs. averaging time (τ). The runs are identified by the symbols in Table I. Wind parallel to path.

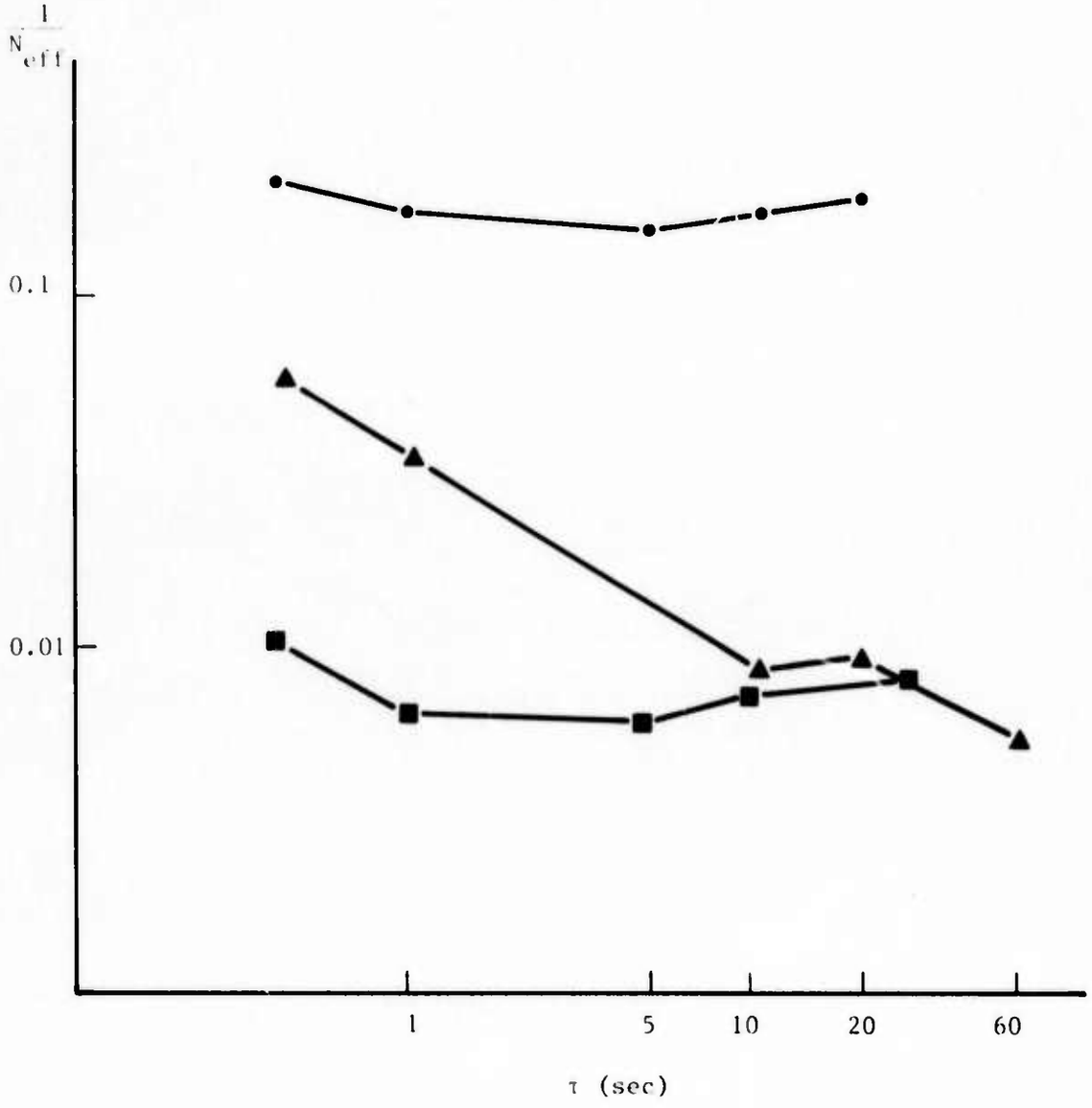

Figure 1b. The reciprocal number of effectively-independent turbulence regions $\left(\frac{1}{N_{eff}}\right)$ along a propagation path, vs. averaging time (τ). The runs are identified by the sumbols in Table I. Wind components normal to the path.

We now examine the results for Var $C_{n_\tau}^2$ alone (Fig. 2a). The slopes are in general less than the expected value of (minus) one, suggesting that τ is not in general >> $I_{\Delta T^2}$. If the wind speed is v, the value of $vI_{\Delta T^2}$ is a function of the degree of spatial intermittency of the turbulence (Ref. 1), and in some of the curves may be indicated by a breakpoint in Fig. 2a.

The results for Var σ_τ^2 likewise do not show the simple behavior of the idealized model (Fig. 2b). We point out three complicating factors:

1. A real wind field may be expected to be irregular over the scales of interest here, so that regions of given turbulence strength are not "frozen-in". This will cause a tendency for a (-1) rather than (0) slope for parallel wind in Fig. 2b.
2. If τ is not >> $I_{\Delta T^2}$, or if there are large-scale correlations for low spatial frequencies in ΔT^2, the slopes in Fig. 2b will tend towards zero. This will be especially noticeable for transverse wind, where they would otherwise be (-1), and this is evident for runs 7 and 9.
3. For small τ ($<<I_{\Delta T^2}$) on the scale of the actual scintillations themselves, Eq. 14a of Ref. 1 will apply, and slopes will tend to (-1) as in Fig. 2b. However, these shorter averaging times are not generally useful for indications of C_n^2 or σ^2.

B. Microthermal Envelope Correlations

These subtleties can be further explored using spaced microthermal-probe-pair measurements of C_n^2 correlations vs. averaging time. The measurement scheme is described in Fig. 13 of Ref. 1. In Figs. 3a, b correlations of the mean-square fluctuations $\overline{\Delta T^2}|_\tau$ ($\sim C_{n_\tau}^2$) are given for three values of τ, for separations nearly parallel to the wind direction (the line along which the respective probe pairs are situated is slightly offset from the wind vector to preclude wake effects from the instruments). The basic spatial integral scale of ΔT^2 can be deduced from the lowest or τ = 0.4 sec curve, and the tendency of the integral scale to become equal to $v\,\tau/2$ for larger τ is evident from the other two curves.

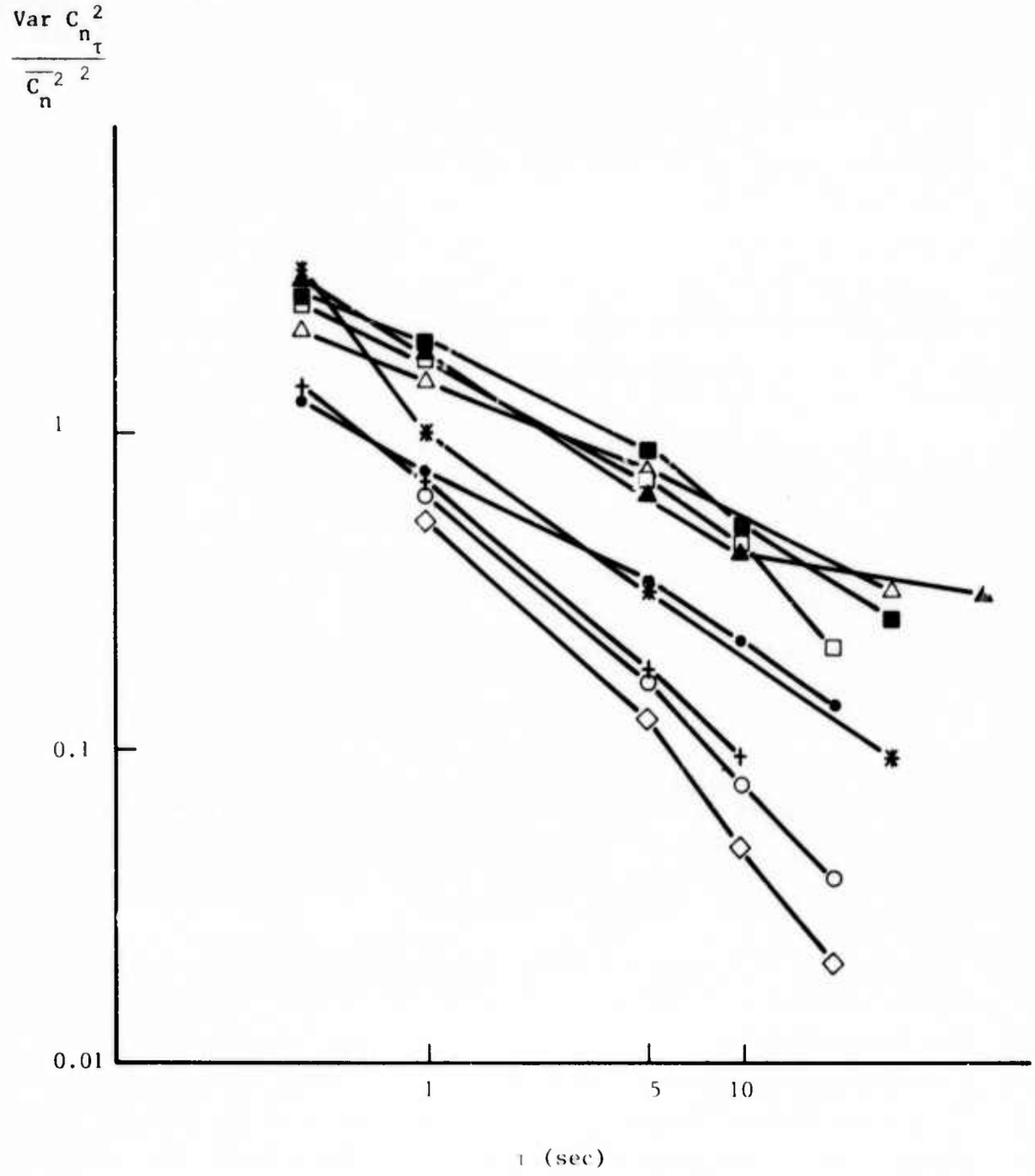

Figure 2a. Normalized variance (spread) of measurements of strength of microthermal and optical fluctuations, vs. averaging time (τ). Microthermal case ($C_{n_\tau}^2$).

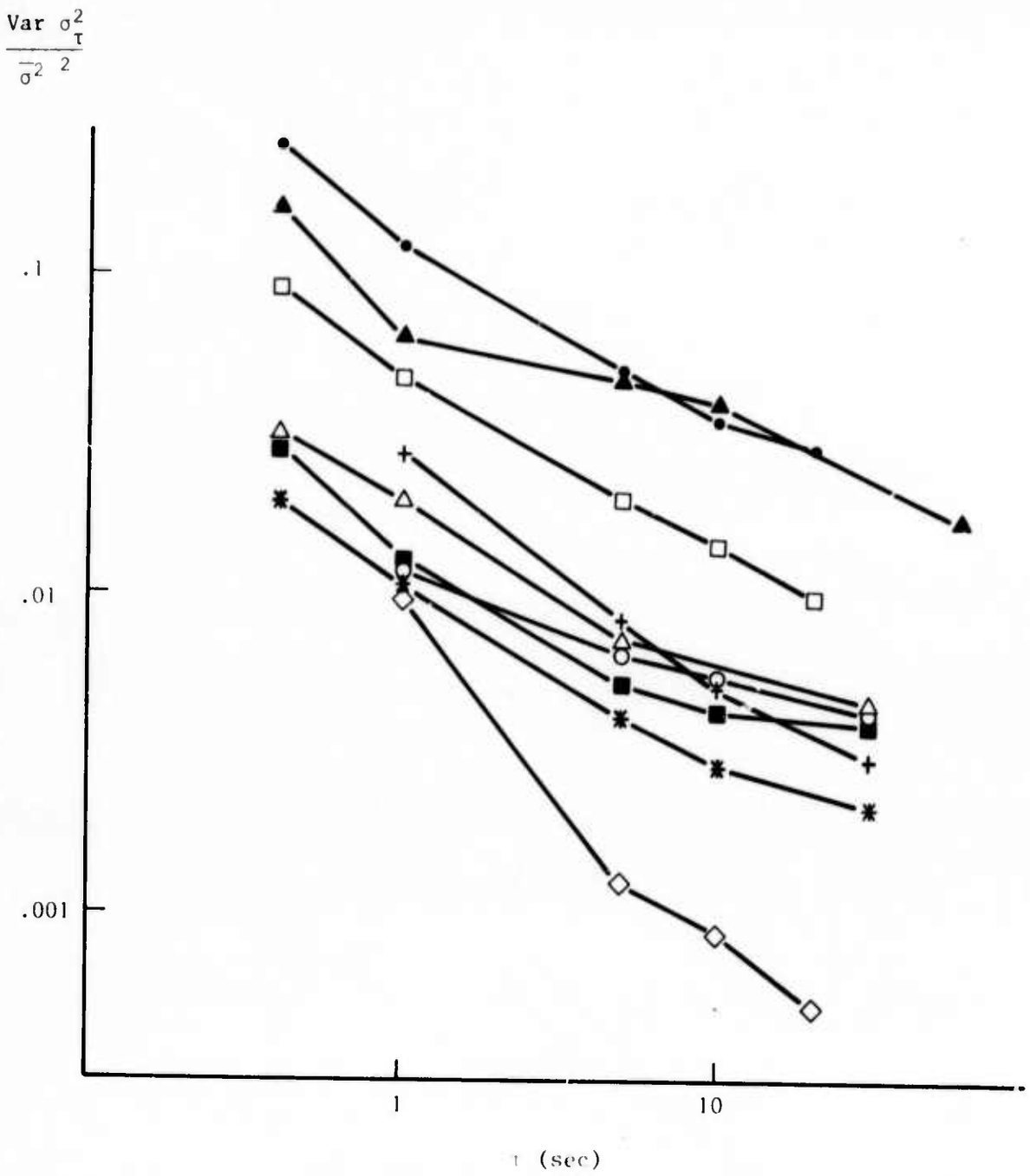

Figure 2b. Normalized variance (spread) of measurements of strength of microthermal and optical fluctuations, vs. averaging time (τ). Optical (log amplitude) scintillations (σ^2_τ).

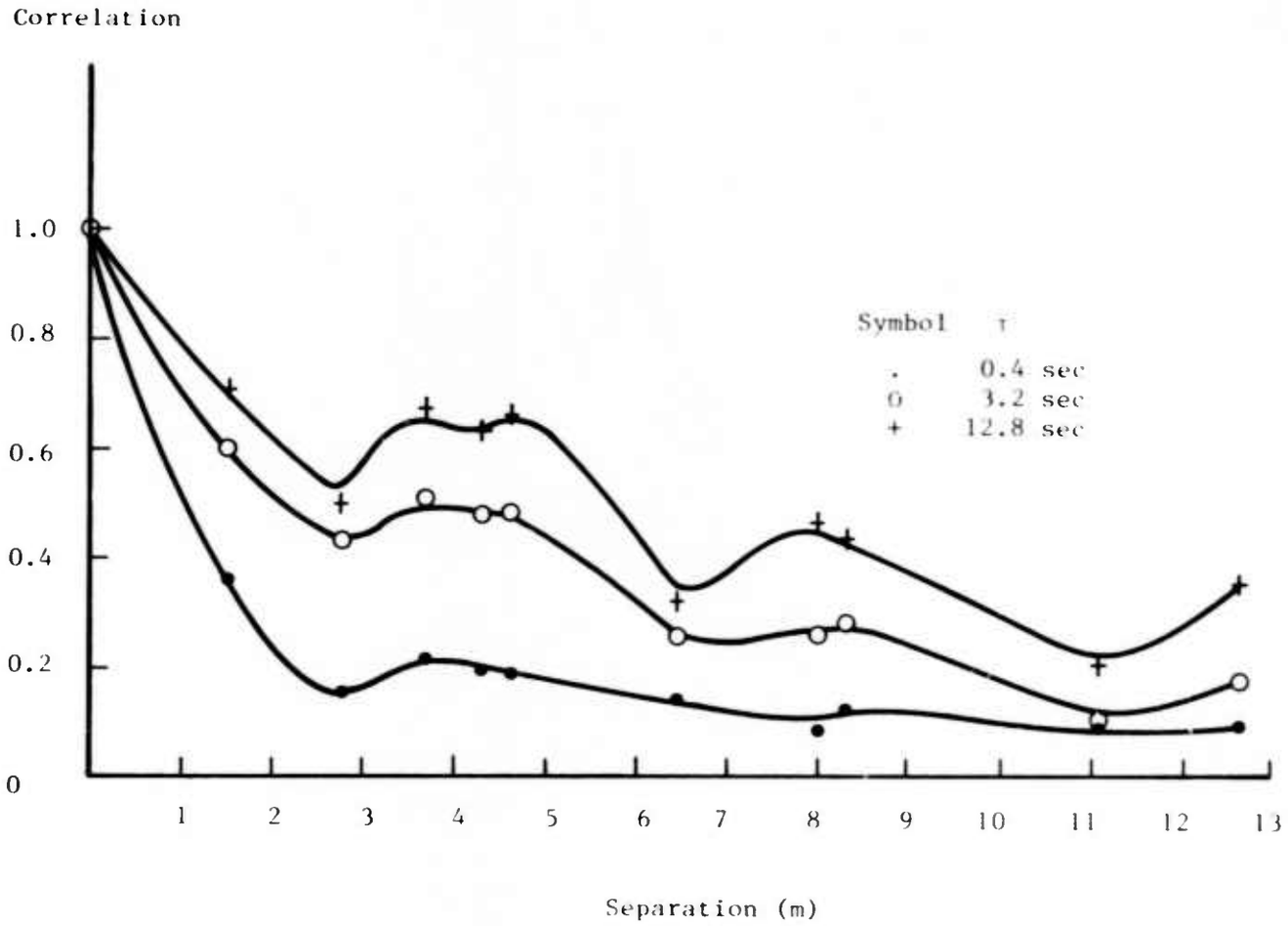

Figure 3a. Microthermal-envelope or strength-of-turbulence spatial correlations vs. separation in a direction parallel to the wind, for three values of averaging time (τ).
Wind speed 1.5 m/sec.

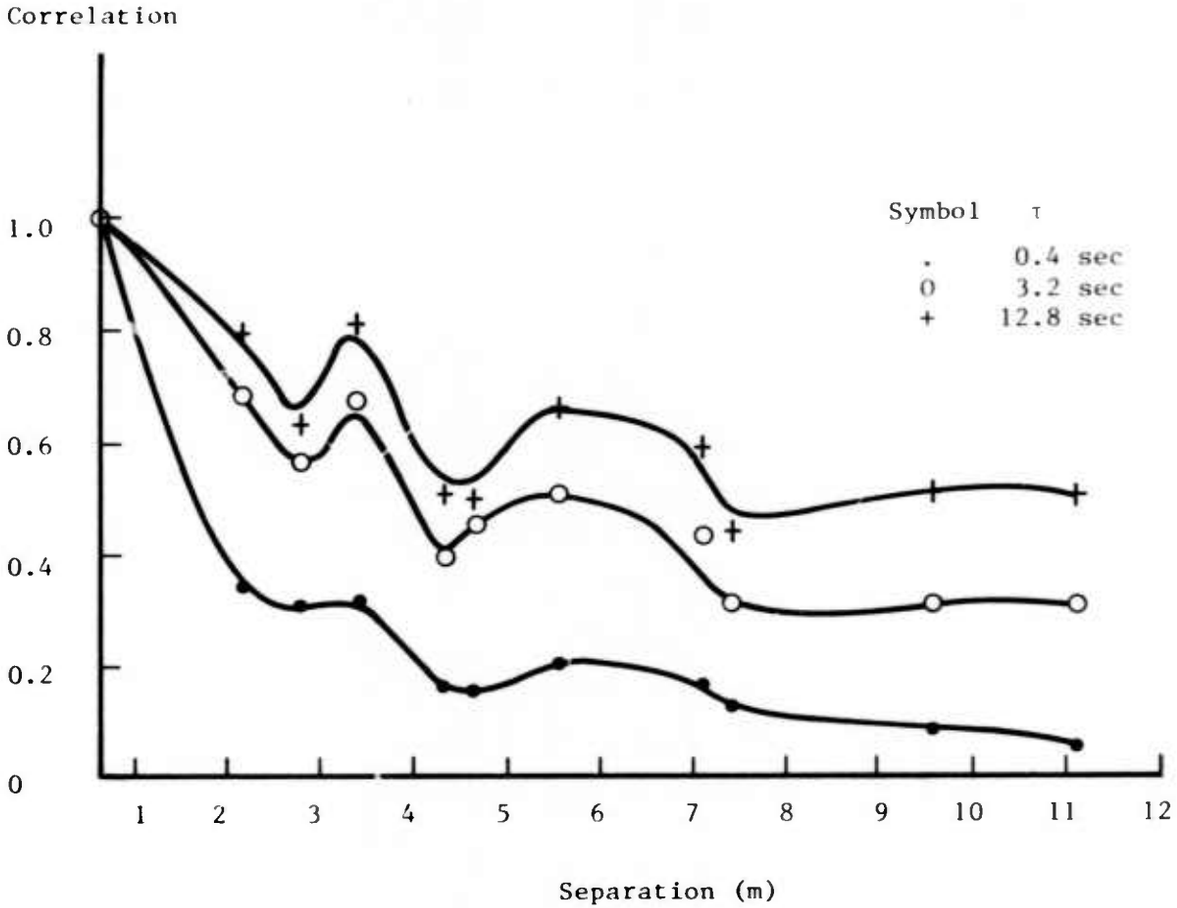

Figure 3b. Microthermal-envelope or strength-of-turbulence spatial correlations vs. separation in a direction parallel to the wind, for three values of averaging time (τ).
Wind speed 4.6 m/sec.

Similar curves for a transverse wind are given in Figs. 4a, b. The tendency for the large-τ curve to decorrelate at larger separations is evident in Fig. 4b. In Fig. 4a, an anomaly is observed whereby the basic squared-microthermal-fluctuations exhibit a correlation tail at large separations, which is also manifested in the large-τ case.

C. A Quantitative View of Turbulence Intermittency

A simple operational measure of the "intermittency" of turbulence is

$$R = \frac{\text{Standard Deviation for } C_{n_\tau}^2}{\overline{C_n^2}} \quad , \qquad (5)$$

where τ may be taken as e.g. 10 seconds. In Figure 5 we show differential probe measurements of ΔT for values of R of 0.46 and 0.68, which might be described as intermediate and pronounced intermittency, respectively.

In Table II, data ranging from cases of light intermittency (R = 0.26) to heavy intermittency (R = 0.77) are shown. The integral scale of ΔT^2 after filtering or smoothing with τ = 1 sec, is the integral of the autocorrelation function of this smoothed process; it is seen to increase with increased intermittency, as expected, and decreases toward $\tau/2$ only for light intermittency. This indicates that intermittency does indeed introduce a long tail in the correlation function of the basic, unfiltered (ΔT^2) process. Similarly, the flatness factor $\beta_{2_{\Delta T}}$ (Ref. 1) associated with the probability distribution of the unfiltered fluctuations is seen to be much higher in the intermittent case, directly indicating the predominance of occasional excursions of extreme magnitude in that case. It may be also noted that intermittency is generally associated with low-wind, poorly-mixed conditions characterized by occasional "bursts" of turbulence.

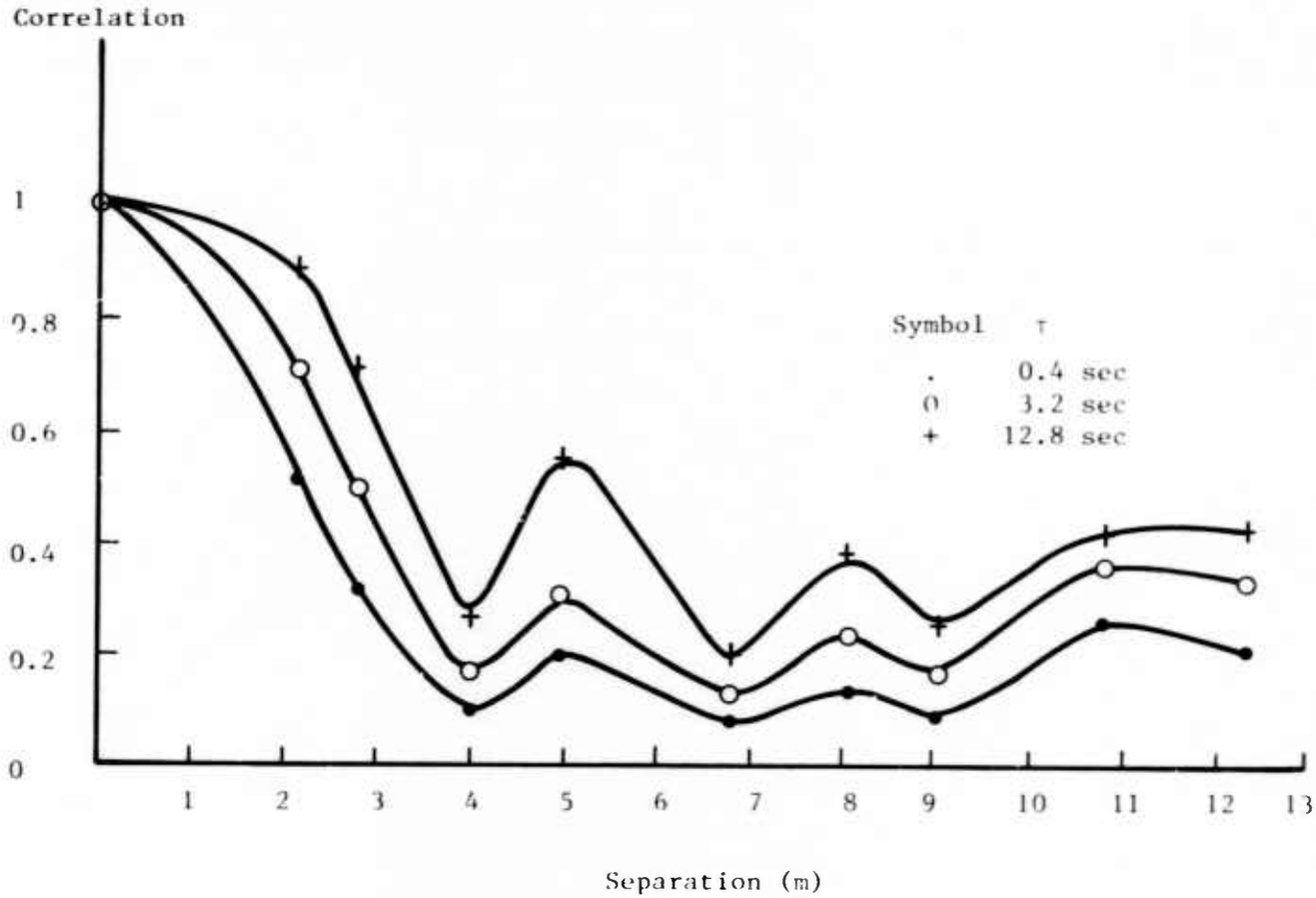

Figure 4a . Microthermal-envelope or strength-of-turbulence spatial correlations vs. separation in a direction perpendicular to the wind, for three values of averaging time (τ).
Wind speed 0.91 m/sec.

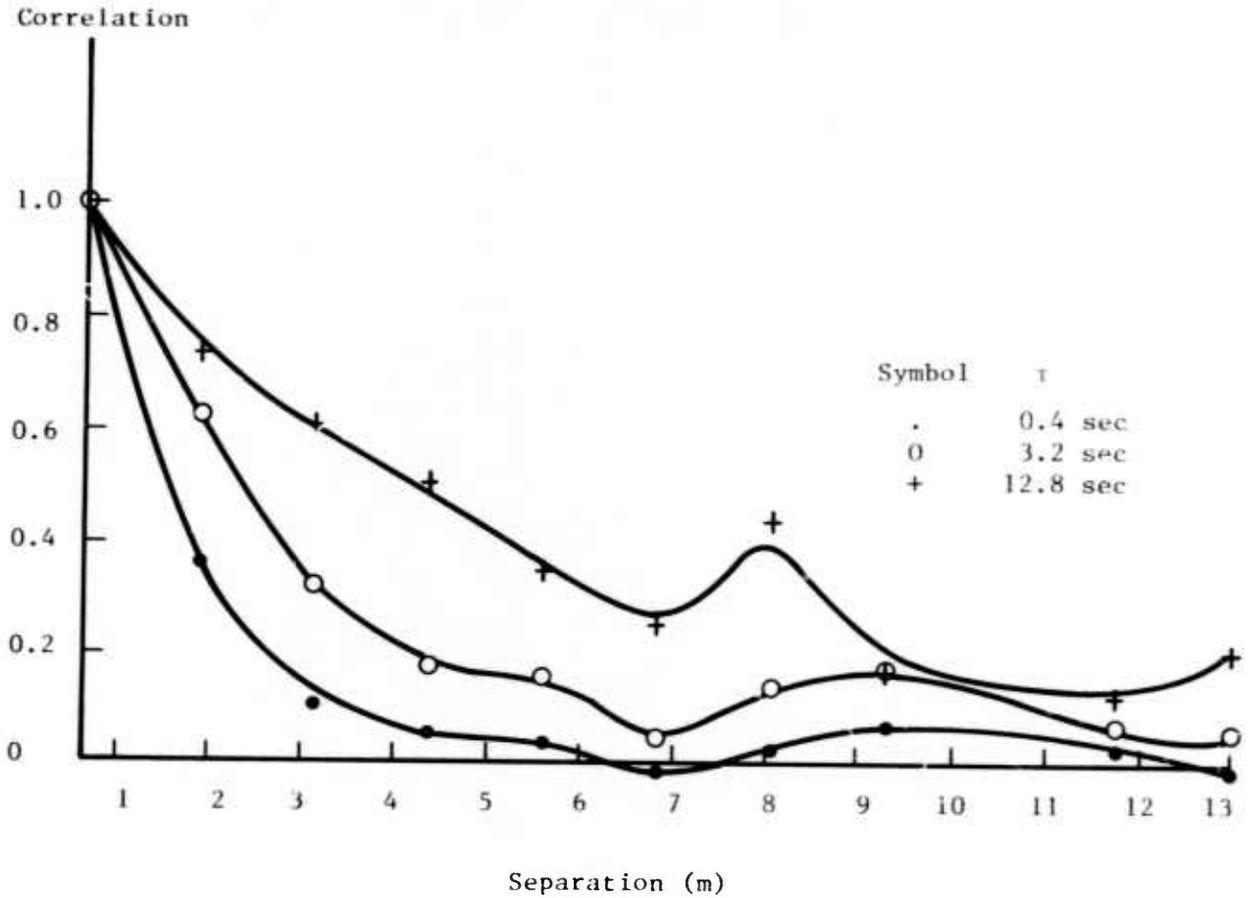

Figure 4b. Microthermal-envelope or strength-of-turbulence spatial correlations vs. separation in a direction perpendicular to the wind, for three values of averaging time (τ).
Wind speed 1.5 m/sec.

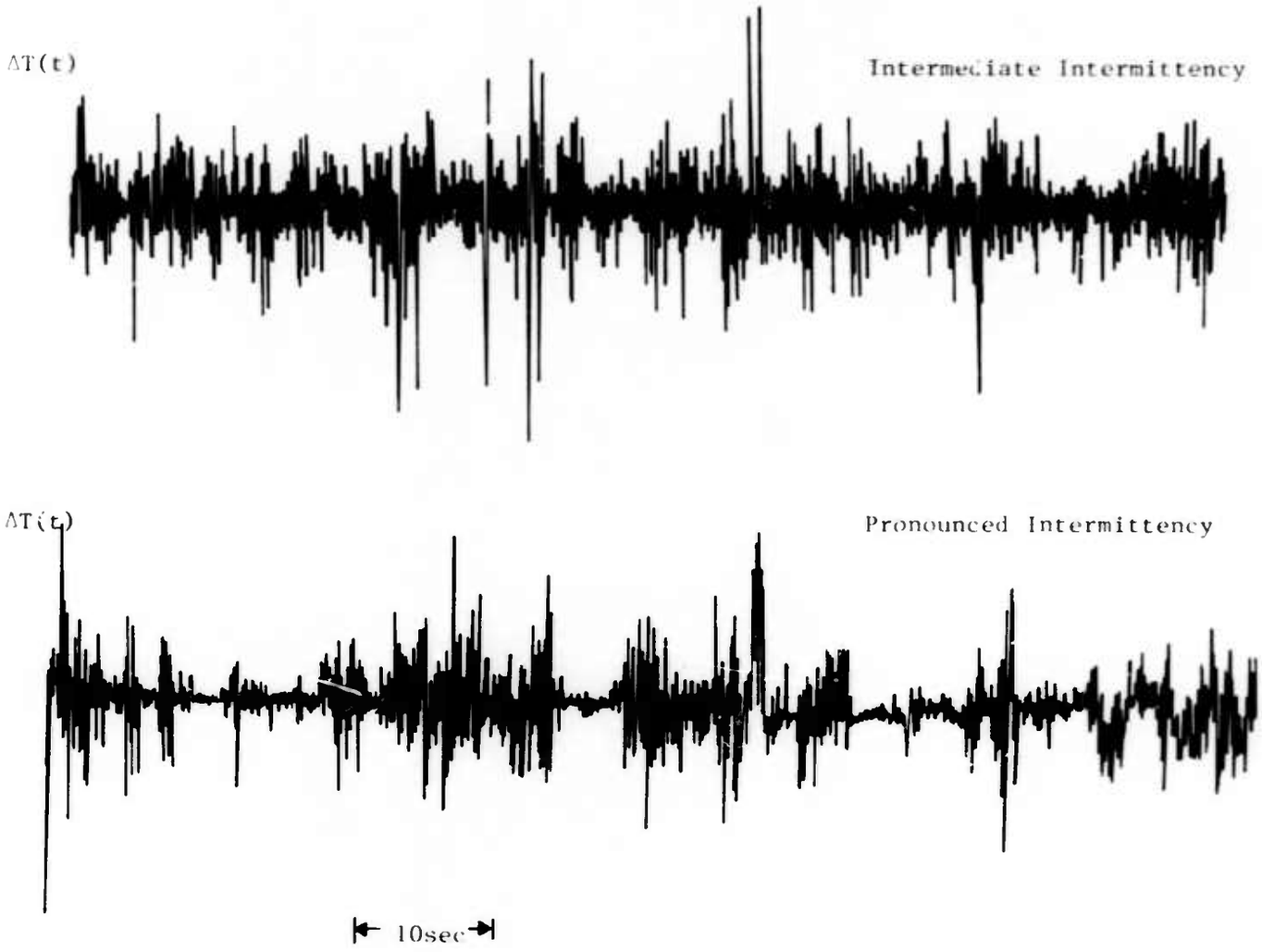

Figure 5. Differential probe measurements of microthermal fluctuations ΔT(t), indicating conditions of intermediate and pronounced intermittency of turbulence.

TABLE I.

Wind Speed (v)	$R = \frac{\text{S.D. } C_{n_\tau}^2 = 10 \text{ sec.}}{\overline{C_n^2}}$	Int. Scale ΔT^2 τ = 1 sec	Corr. Length $v \cdot I_{\Delta T^2}$	$\beta_{2\ \Delta T}$
(m/sec)		(sec)	(m)	
9	.270	0.8	7.2	5.5
5.5	.261	1.38	7.6	8.35
4.5	.457	1.47	6.6	11.15
3.8	.468	1.49	5.7	13.4
1.5	.767	3.48	5.2	12.32

III. CONDITIONAL FADING STATISTICS

A topic related to the short-term considerations discussed previously is that of the conditional statistics of scintillation or irradiance fluctuations. The applications of this concept include "pilot-tone" or burst communications systems in which the channel is monitored and used only when it is "good", and target illumination systems in which e.g. a high-power laser is utilized immediately after a low-power laser (or some other channel monitoring scheme) indicates a favorable short-term path. The applicable question may be posed as follows: given that the instantaneous target irradiance is above some predetermined threshold, what is the probability distribution of the irradiance at an arbitrary time τ later? The present discussion is limited to the linear propagation case.

A. Analysis of the Conditional Problem

In previous work on this program, it has been determined that scintillation does not constitute a Markov process. It has been determined by ourselves and a number of other investigators, however, that this phenomenon is for most practical purposes log-normally-distributed. To the extent that we can assume that the two-point log distribution is bivariate normal, the problem is readily tractable.[2] However, we point out that the conditional statistics can be very sensitive to departures from this distribution and theoretical arguments suggest that exact log normality is not even possible for the one-point distribution.[3] Furthermore, as described below, our preliminary analysis of experimental data shows significant departure of the two-point distribution from the normal under conditions of strong scintillation.

Nevertheless, the basic approach given here to the conditional problem can be numerically extended to utilize any (non-gaussian) joint

---

2. S. O. Rice, "Mathematical Analysis of Random Noise", in Selected Papers on Noise and Stochastic Processes, N. Wax., ed., Dover Publications, Inc., N.Y., 1954.

3. J. W. Strohbehn, T. Wang, J. P. Speck, Radio Science 10, 59-70, January 1975.

probability distribution which may be empirically or otherwise determined. We will confine this discussion to the log-normal case for simplicity, and empirical verification under certain conditions will be given below.

Let us therefore assume that the two-point or joint probability distribution of the log irradiance is bivariace normal. The important parameter is the correlation coefficient $\rho(\tau)$, which is a function of the time delay τ separating the initial and final observations of the irradiance. The joint distribution of the log irradiance χ is

$$\Pr(\chi(t),\chi(t+\tau)) = \frac{1}{2\pi\sigma_o^2(1-\rho^2(\tau))^{1/2}} \exp\left\{-\frac{1.}{2\sigma_o^2(1-\rho^2(\tau))}\right.$$

$$\left.\cdot\left(\chi^2(t) - 2\rho(\tau)\chi(t)\chi(t+\tau) + \chi^2(t+\tau)\right)\right\} \quad (6)$$

where χ is normally distributed with variance σ_o^2 and zero mean, and

$$\rho(\tau) \equiv \frac{\langle\chi(t)\chi(t+\tau)\rangle}{\sigma_o^2} \quad .$$

The conditional distribution of $\chi(t+\tau)$, given that $\chi(t) = L$, is

$$\Pr(\chi(t+\tau)\,|\,\chi(t) = L) = \frac{1}{\sqrt{2\pi}\sigma_o(1-\rho^2(t))^{1/2}} \exp\left\{\frac{-1}{2\sigma_o^2(1-\rho^2(\tau))}\right.$$

$$\left.\cdot(\chi(t+\tau) - \rho(\tau)L)^2\right\} \quad (7)$$

which is normal with the following mean and variance:

$$\text{Mean} = L\rho(\tau)$$
$$\text{Var} = \sigma_o^2 (1-\rho^2(\tau)) \quad . \tag{8}$$

We are now interested in the probability that $\chi(t + \tau)$ is less than a fixed "fade" level (ℓ_1), given that $\chi(t)$ exceeds a threshold "pilot level" (ℓ_o):

$$\Pr(\chi(t + \tau) \leq \ell_1 \mid \chi(t) \geq \ell_o) = \int_{\ell_o}^{\infty} d\chi(t) \int_{-\infty}^{\ell_1} d(\chi(t + \tau))\ P(\chi(t),\chi(t+\tau))$$

$$: \int_{\ell_o}^{\infty} d\chi \quad \frac{1}{\sigma\sqrt{2\pi}} \quad e^{\frac{-\chi^2}{2\sigma^2}} \tag{9}$$

We define the following quantities:[4]

$$Z(x) \equiv \frac{1}{\sqrt{2\pi}} \quad e^{-x^2/2} \tag{9a}$$

$$P(x) \equiv \int_{-\infty}^{x} Z(t)dt \tag{9b}$$

$$Q(x) \equiv \int_{x}^{\infty} Z(t)dt \tag{9c}$$

---

4. M. Abramowitz and I. Stegun, ed., Handbook of Mathematical Functions, Dover Publications, Inc., N.Y. 931-940, 1965.

$$g(x,y,\rho) = (2\pi\sqrt{1-\rho^2})^{-1} \exp\left[-\frac{1}{2(1-\rho^2)} (x^2-2\rho xy + y^2) \right] \tag{9d}$$

$$L(h,k,\rho) = \int_h^\infty dx \int_k^\infty dy\ g(x,y,\rho) \tag{9e}$$

We note that

$$P(x) + Q(x) = 1 \tag{10a}$$

$$P(-x) = Q(x) \tag{10b}$$

$$L(h,-k,-\rho) = \int_h^\infty dx \int_{-\infty}^k dy\ g(x,y,\rho) \tag{10c}$$

With these definitions, we have

$$\Pr(\chi(t+\tau) \leq \ell_1 | \chi(t) \geq \ell_o) = L\left(\frac{\ell_o}{\sigma_o}, \frac{-\ell_1}{\sigma_o}, -\rho\right) / Q\left(\frac{\ell_o}{\sigma_o}\right)$$

$$= L\left(\frac{\ell_o}{\sigma_o}, \frac{-\ell_1}{\sigma_o}, -\rho\right) / P\left(\frac{-\ell_o}{\sigma_o}\right) \tag{11}$$

This expression must be evaluated numerically for various values of ℓ_o, ℓ_1, σ_o, and ρ. The calculation is expedited by use of the formula

$$L(h,k,\rho) = Q(h)Q(k) + \sum_{\eta=o}^{\infty} \frac{Z^{(\eta)}(h)Z^{(\eta)}(k)}{(\eta + 1)!} \rho^{\eta + 1} \qquad (12)$$

where

$$Z^{(\eta)}(x) = \frac{d^{\eta}}{dx^{\eta}} Z(x) = -xZ^{(\eta - 1)}(x) - (\eta - 1) Z^{(\eta - 2)}(x) \qquad (13)$$

In practice, in the worst cases about 50 terms must be retained in the sum for the accuracy to be better than 1×10^{-6}.

We have performed computer runs for several different pilot and fade levels, using correlation functions (Fig. 6,6a) obtained empirically under three different scintillation conditions at 10.6μ:

	Strength of Scintillation	Wind Speed	Symbol
Run A	$\sigma_o^2/4 = 0.307$	1 m/s variable	A
Run B	$\sigma_o^2/4 = 0.010$	3.5 m/s at 45° to path	Θ
Run C	$\sigma_o^2/4 = 0.0015$	9 m/s at 45° to path	X

The pilot and fade levels are conveniently normalized by the mean irradiance $\bar{I}$. We thus calculate the probability that $\ln\left[I(\tau)/\bar{I}\right] \leq \ln(I_1/\bar{I})$ given that $\ln\left[I(0)/\bar{I}\right] \geq \ln(I_o/\bar{I})$, for particular correlation functions and values of σ_o^2, I_1, I_o.

The results for strong scintillations (Run A), a fade level of 0.5 $\bar{I}$, and six pilot levels are shown in Fig. 7. It is apparent that, for this particular correlation function, indicative of a low wind condition and strong scintillation, a conditioning or pilot threshold of 0.95 $\bar{I}$ results in a less than 5% probability that the irradiance will fall below 0.5 $\bar{I}$ until 18 msec later. If the conditioning threshold is

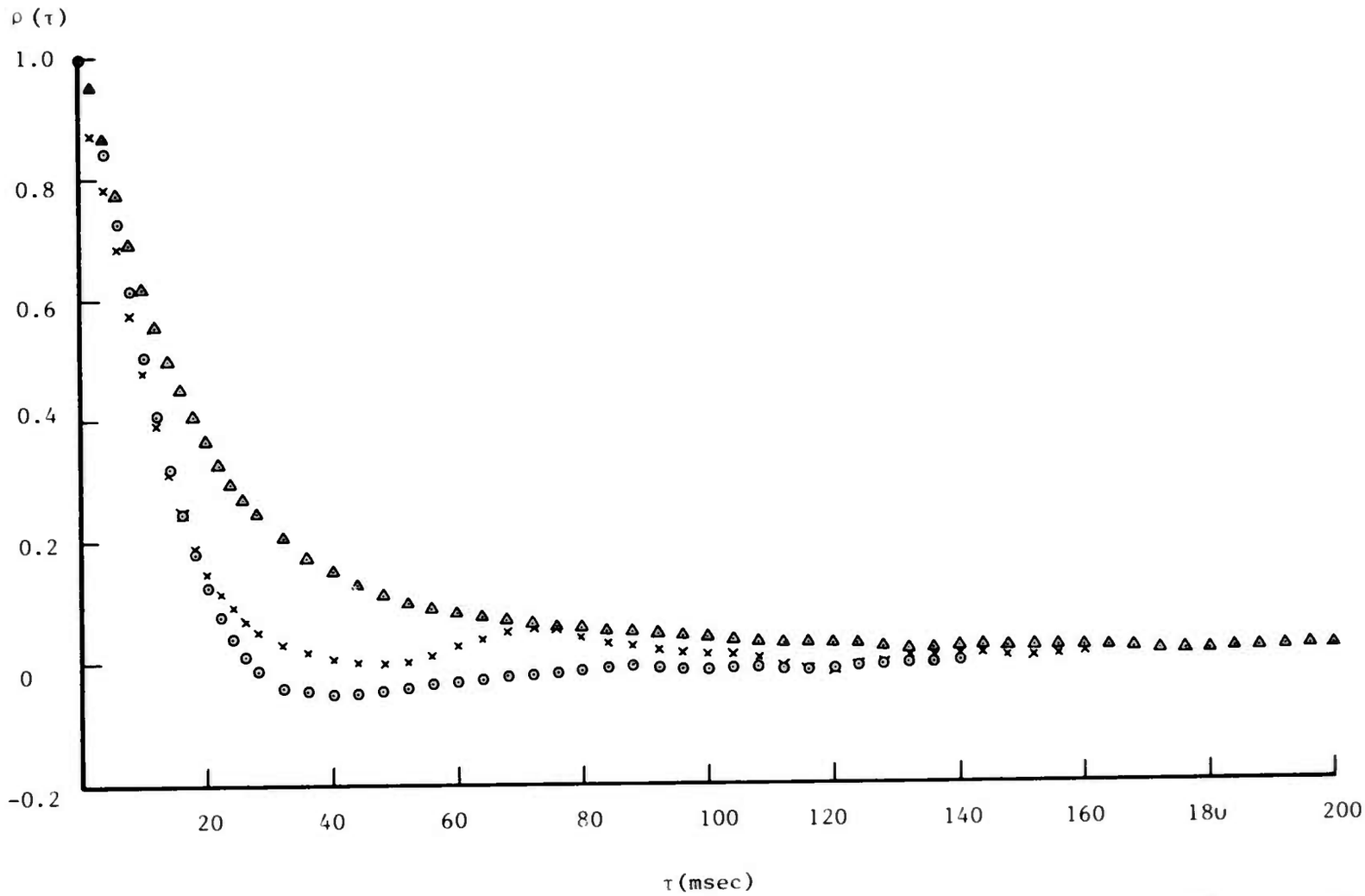

Figure 6. Empirical, two-point temporal correlation functions (ρ) for log irradiance scintillations, vs. delay time (τ).

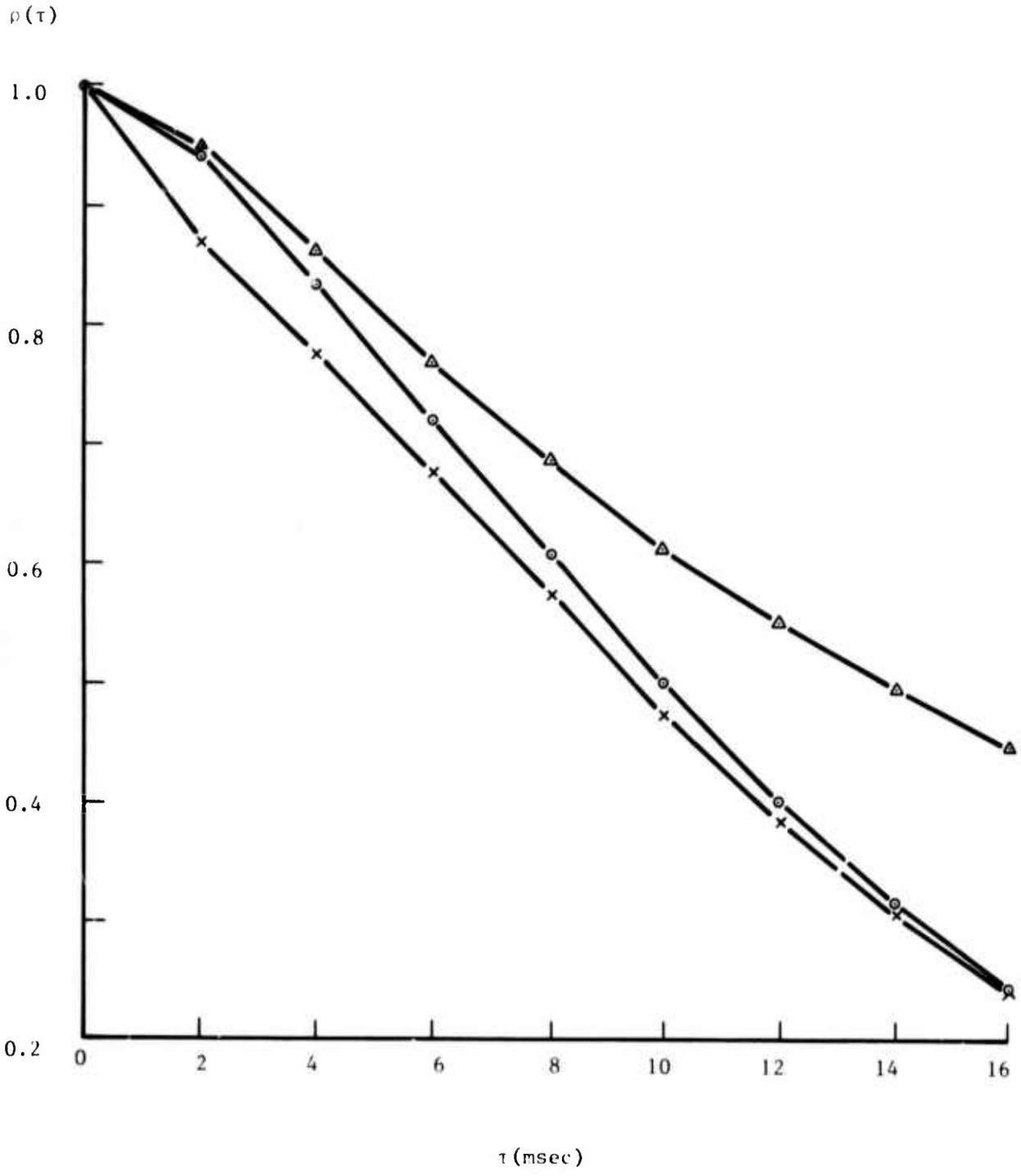

Figure 6a. Expanded detail for Fig. 6 at small delays (τ).

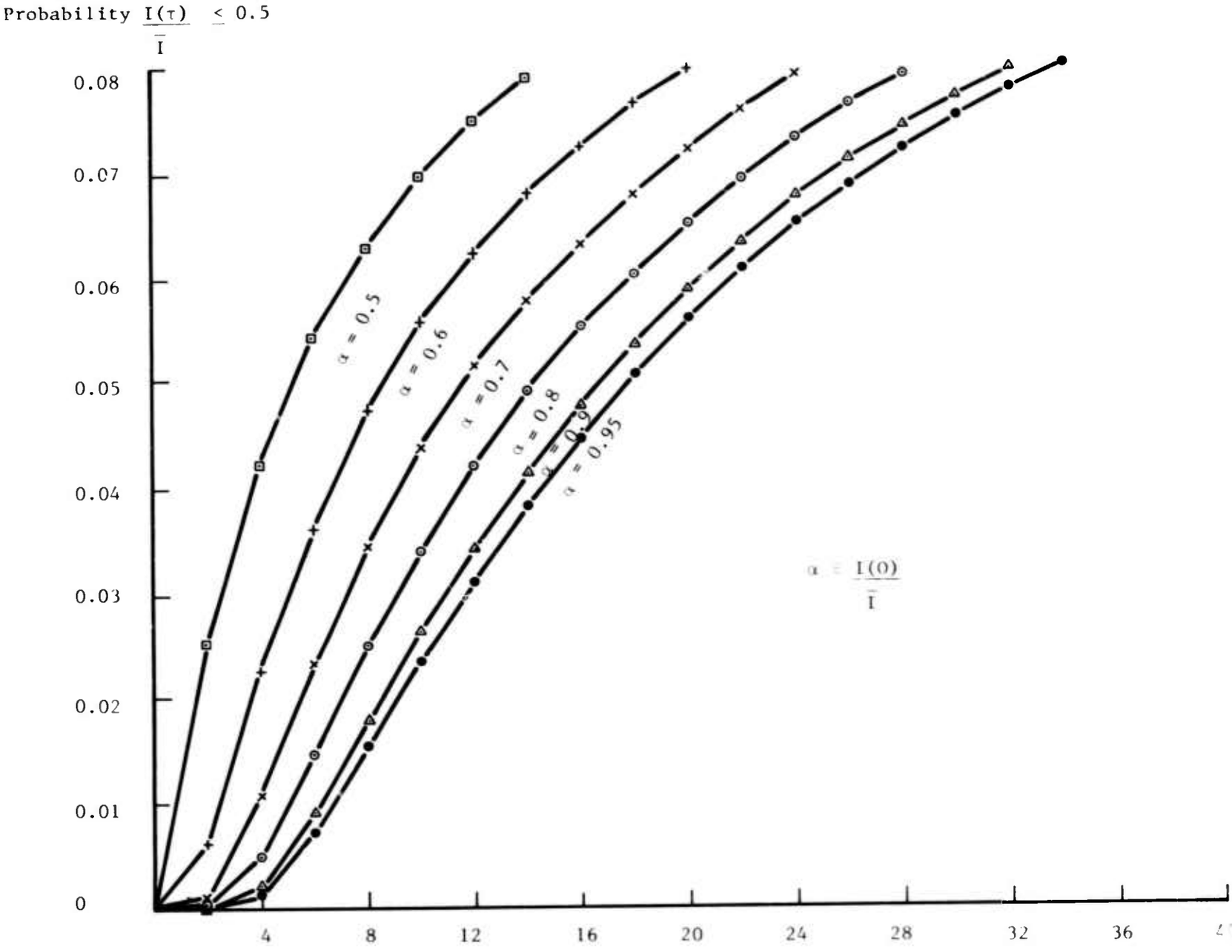

Figure 7. The probability that irradiance $I(\tau)$ at time $t = \tau$ will be $\leq$ half the mean irradiance ($\bar{I}$), given that it is $\geq \alpha \bar{I}$ at $t = 0$, vs. τ (Run A). Six values of the parameter α are shown.

0.5 $\bar{I}$, the corresponding time interval is 5 msec. As the threshold is made lower, it will be reached more often, but the following time interval for favorable propagation conditions will be correspondingly shorter. For instance, for a threshold of 0.7 $\bar{I}$, which is exceeded 74% of the time, and a time interval of 1 msec, the fade level will fall below 0.5 $\bar{I}$ only once in 1,000 times. This approach obviously yields sufficient information for an analysis of use-rate vs. reliability.

B. Test of the Bivariate Normal Distribution

The degree to which the empirical scintillation data agree with the above assumption of two-point bivariate normality for the log irradiance is being investigated for a number of runs. For example, for the weak scintillation case of Run C, the one-point log distribution (Fig. 8) has an observed skewness of 0.05 and kurtosis of 3.1. Table III shows the skewness and kurtosis of the conditional distributions vs. τ and the pilot level ℓ_o, where χ and ℓ_o have been normalized by the standard deviation σ_o. The distributions indicate normality except for small τ and $\frac{\ell_o}{\sigma_o} = -1$. Three of these conditional distributions are shown in Fig. 9. Using measured values of the correlation function for this run (Table IV), we compare the predicted, normalized conditional mean and variance (Eq. 8) with observed values, in Tables V and VI. Excellent agreement with the gaussian assumption is evident.

Under conditions of strong scintillation, e.g. Run A above, there is evidence of appreciable departure from the bivariate normal distribution. This is under further investigation.

IV. NEW EXPERIMENTAL WORK AND FACILITIES

A. Target Irradiance Statistics with Beam Wander Cancellation

In preceding reports on this program (Refs. 1,5), analytical results were given for the mean target irradiance and its fluctuations resulting from the effects of turbulence on a finite beam wave, including the cancellation of turbulence-induced beam wander. Experimental results were given for a 1.6 km path operating at 6328Å with a wander-cancelling tracker.

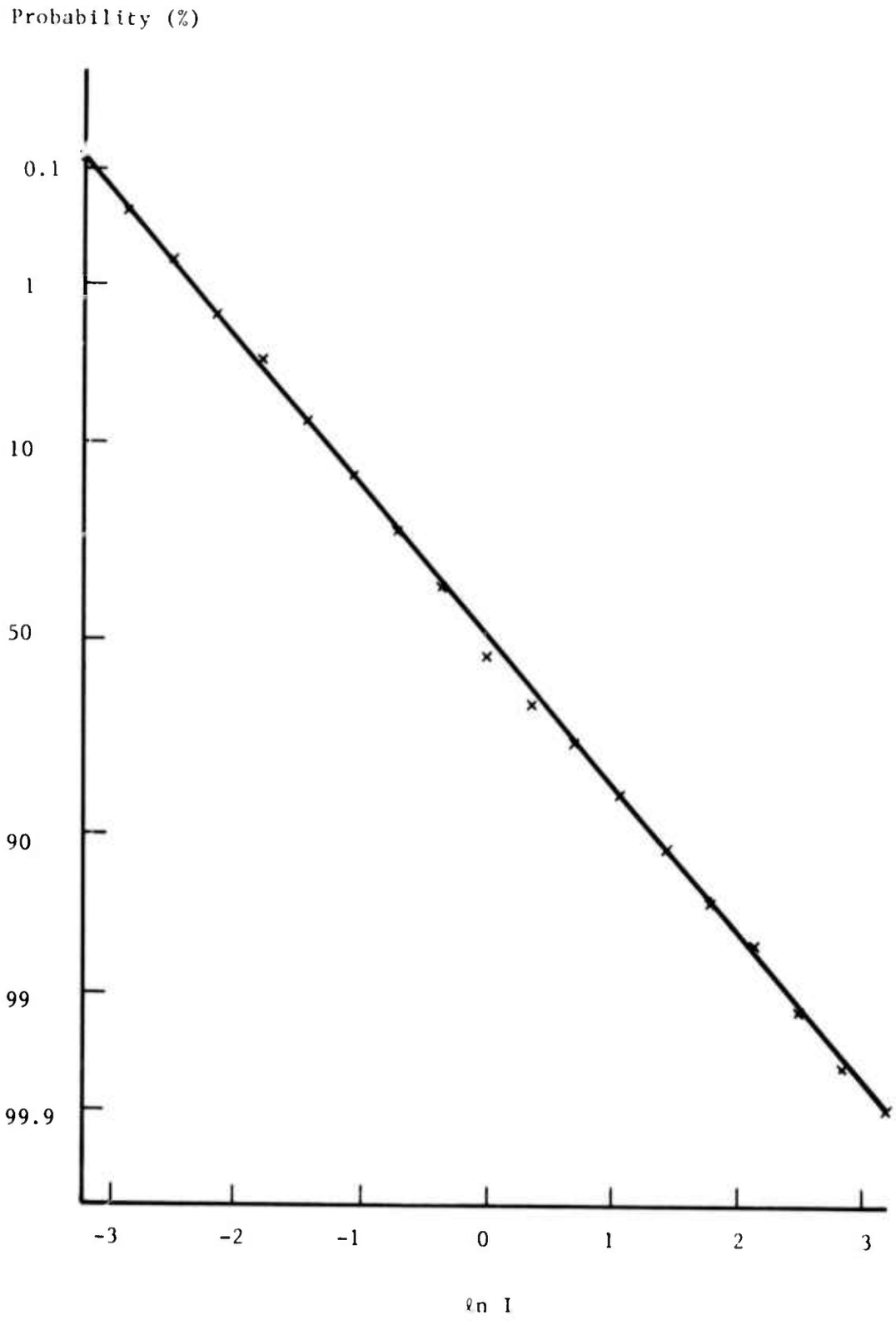

Figure 8. One-point probability distribution of log irradiance for Run C.

TABLE III

Skewness (S) and Kurtosis (K) of $Pr(\chi(t + \tau)|\chi(t))$ for Run C

S

ℓ_o/σ_o \ τ(ms)	1	2	4	8	16
-1	.29	.13	.2	.022	.012
0	.03	.051	.056	.061	.068
1	-.12	-.017	.01	.13	-.055
2	-.0039	.047	.0080	-.0065	-.036

K

ℓ_o/σ_o \ τ(ms)	1	2	4	8	16
-1	4.2	3.59	3.83	3.29	3.18
0	3.20	3.16	3.089	3.05	3.04
1	3.27	3.21	2.69	2.77	3.17
2	2.83	2.84	2.95	2.98	3.08

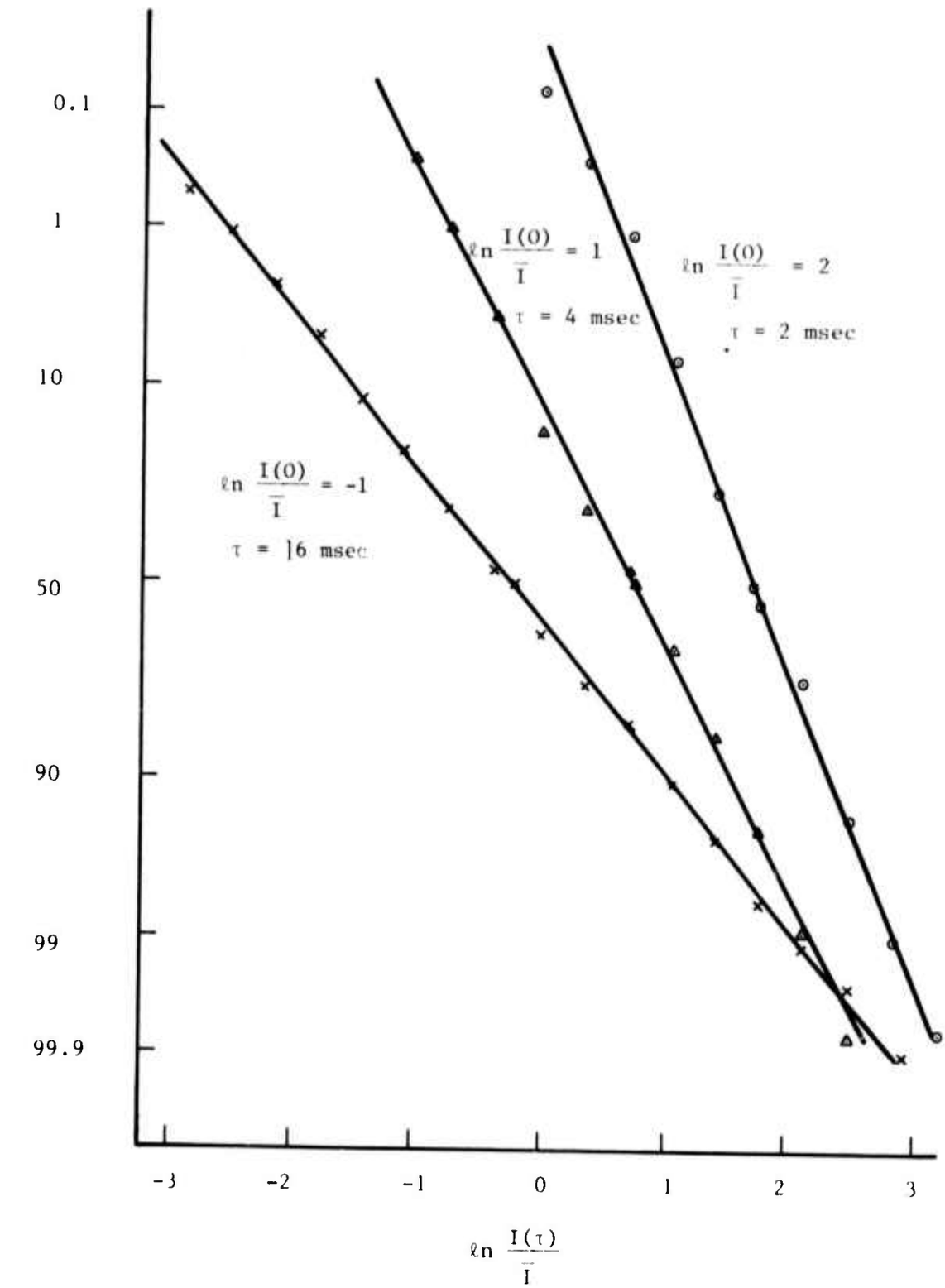

Figure 9 . Conditional probability for normalized log irradiance at time t = τ, given the value at t = 0.

TABLE IV

Correlation Function Values for Run C

τ	$\rho(\tau)$
2 ms	0.87
4 ms	0.78
8 ms	0.57
16 ms	0.24

TABLE V

Comparison of Predicted and Observed Mean of $\Pr\left(\frac{\chi(t+\tau)}{\sigma_o} \middle| \frac{\chi(t)}{\sigma_o} = \frac{\ell_o}{\sigma_o}\right)$ For Run C

$\frac{\ell_o}{\sigma_o}$ \ τ ms		2	4	8	16
-1	Predicted	-0.87	-0.78	-0.57	-0.24
	Observed	-0.89	-0.75	-0.60	-0.24
0	Predicted	0	0	0	0
	Observed	-0.016	-0.016	-0.001	0.008
1	Predicted	0.87	0.78	0.57	0.24
	Observed	0.85	0.72	0 50	0.21
2	Predicted	1.74	1.56	1.14	0.48
	Observed	1.70	1.51	1.09	0.45

TABLE VI

Comparison of Predicted and Observed $\frac{\text{Variance}}{\sigma_o^2}$ of $\Pr\left(\frac{\chi(t+\tau)}{\sigma_o} \middle| \frac{\chi(t)}{\sigma_o} = \frac{\ell_o}{\sigma_o}\right)$

For Run C

$\frac{\ell_o}{\sigma_o}$ \ τ ms		2	4	8	16
-1	Predicted	0.243	0.392	0.675	0.942
	Observed	0.239	0.414	0.651	0.936
0	Predicted	0.243	0.392	0.675	0.942
	Observed	0.236	0.406	0.686	0.961
1	Predicted	0.243	0.392	0.675	0.942
	Observed	0.278	0.402	0.77	1.01
2	Predicted	0.243	0.392	0.675	0.942
	Observed	0.254	0.439	0.765	0.99

Following the above experimental effort, the facility was modified for taking similar data over a much shorter path. This was done in order to achieve smaller ratios of transmitter-diameter-to-coherence-scale (D/ρ_o) for stronger, reasonably developed turbulence, while maintaining a sufficient Fresnel number for the transmitter. This case scales to the infrared conditions of interest, and experiments with this facility have been underway for several months.

The facility is currently undergoing a further modification, to add a simultaneous, coincident-beam capability at 10.6μ. The tracker continues to operate off a target-point beacon at 6328Å, but will now control both optical and 10μ beams (Fig. 10). It is expected that the turbulence-induced wander, being a basically geometrical-optics phenomenon,[5] will not undergo significant wavelength dispersion, so that this tracking scheme will effectively remove wander at the infrared wavelength. Operation at 10.6μ will afford a wavelength-scaled test of our analytical results, and will further reduce D/ρ_o in a well developed turbulence. The receiver configuration is shown in Fig. 11, and in the photograph of Fig. 12.

The data capability and experimental parameters of this enlarged system are summarized in Table VII. We also mention that the analysis given in the preceding report,[1] for the on-axis mean irradiance in the limit $\frac{D}{\rho_o} \to \infty$, is being extended to include some details of the complete curve $\left(1 << \frac{D}{\rho_o} < \infty\right)$. This is being accomplished by means of the extended Huygens-Fresnel formulation and an asymptotic expansion in inverse powers of D/ρ_o. This approach is free of the assumptions and approximations of a recent Russian treatment.[6]

B. Long-Path Saturation System

In earlier work on this program,[7] experiments were conducted over the longest, lowest path which can be reasonably achieved in the

---

5. J. R. Kerr and J. R. Dunphy, "Propagation of Multiwavelength Laser Radiation Through Atmospheric Turbulence", RADC-TR-74-183, May 1974.
6. V. A. Banakh, et al, J. Opt. Soc. Am. 64, 516-518, April 1974.
7. J. R. Dunphy and J. R. Kerr, J. Opt. Soc. Am. 63, 981-986, August 1973.

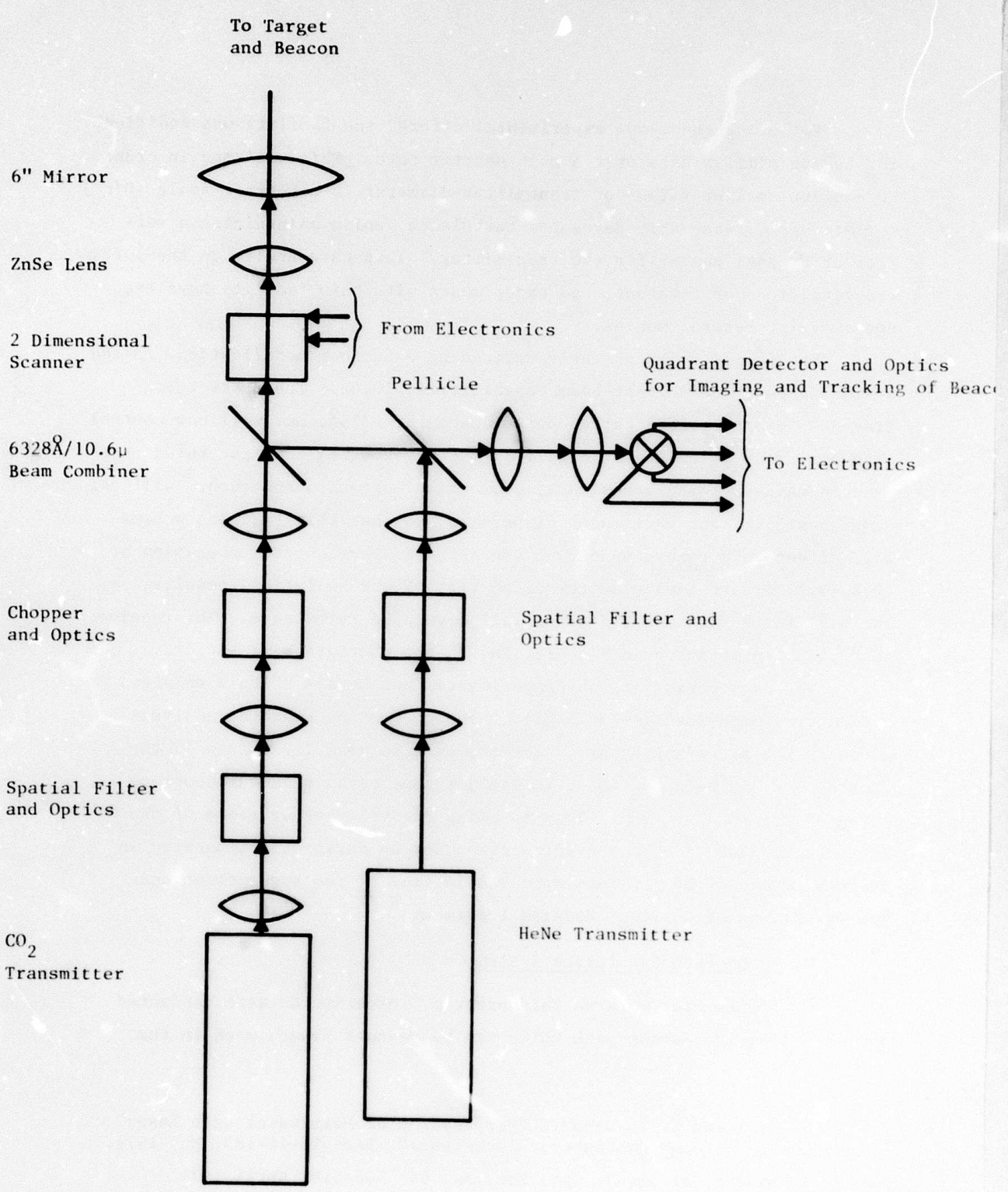

Figure 10. Diagram of multiwavelength tracking transmitter for beam-wander-cancellation and target-irradiance experiments.

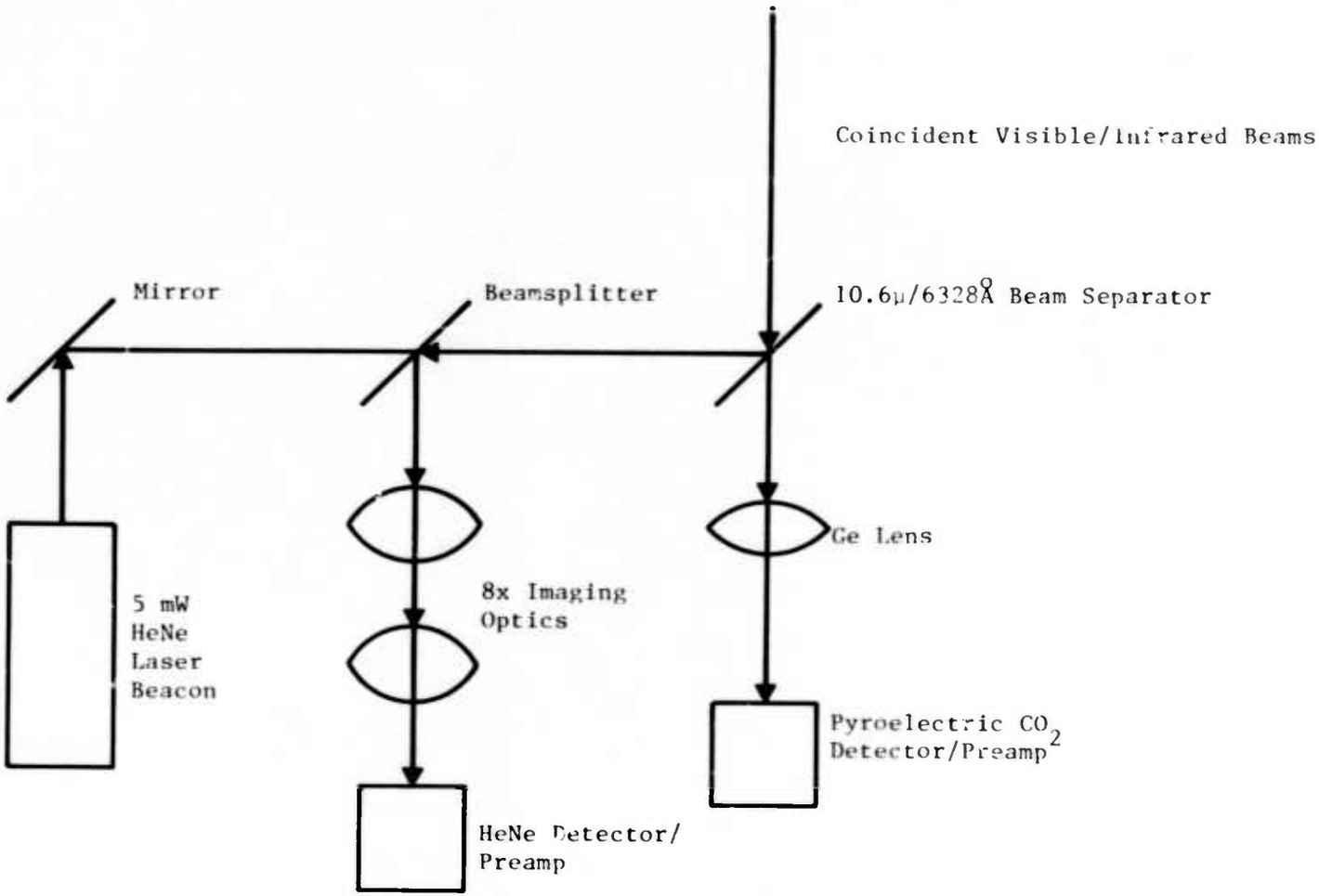

Figure 11. Diagram of multiwavelength receiver for beam-wander-cancellation and target-irradiance experiments.

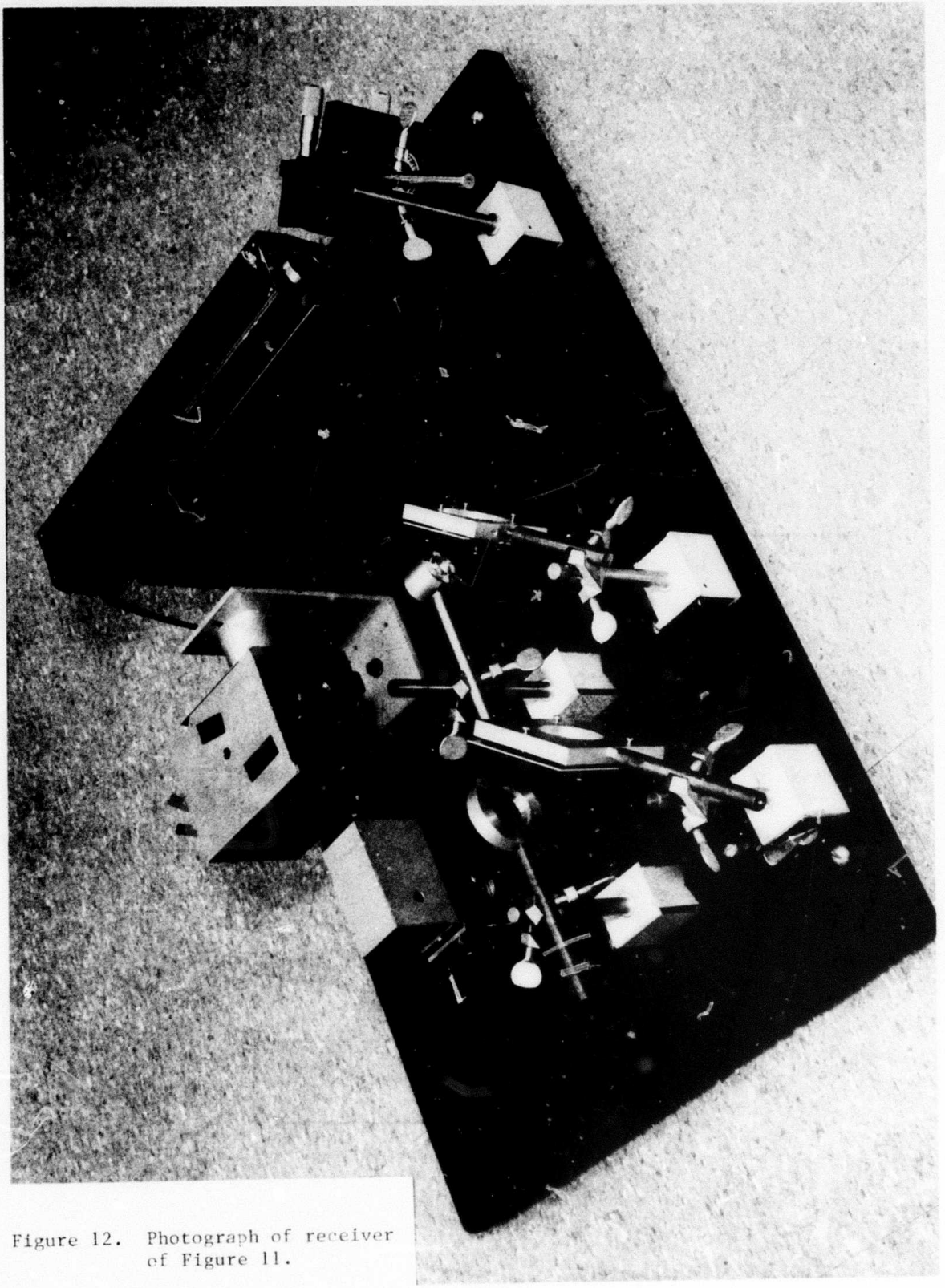

Figure 12. Photograph of receiver of Figure 11.

TABLE VII

Experimental Data and Parameters for Multiwavelength Target-Irradiance System

Tracker:	Wander signals
Target:	Linear irradiance fluctuations Mean linear irradiance Log irradiance fluctuations C_n^2 and microthermal fluctuations Meterological conditions
Processing:	Statistics and spectra of fluctuations

Wavelength: 6328Å and 10.6μ (simultaneous, coincident beams)
Path: 91 m, homogeneous
Beam height: 1.8 m
Mean irradiance: 120 s averaging
Variance { Linear irradiance: 120 s averaging; Log amplitude; Wander angle
Spectra: Digital; 0.1 Hz resolution; 100 s averaging
Analog; 1.0 Hz resolution; 100 s averaging
Probability distributions: Digital
Digital sampling rate: 1 kHz
Target receiver: Quasi-Point-Aperture at each wavelength
Target receiver bandwidth: 1 kHz
Target receiver dynamic range: 80 db at 6328Å; 60db at 10.6μ
Tracking transmitter aperture: 15.2 cm
Tracking transmitter focus resolution: 2.5μm
Steering servo resonant frequency: 300 Hz, no load
Steering servo linearity: <1% of peak-to-peak deflection
Steering servo repeatability: 0.050% of peak-to-peak deflection
Open loop transfer function: Single integration
Closed loop bandwidth: 20 Hz
Noise limited tracking angle: <2% of transmitter diffraction-limited width (6328Å)
Transmitter Chopping: 9kHz at 10.6μ (direct-coupled at 6328Å)
Microthermal probe averaging time: 300 s

presence of earth curvature and atmospheric refraction. In this effort, which was undertaken for a better understanding of strong turbulence scattering ("hard saturation" of scintillations), it was determined that multikilohertz fluctuations and correspondingly small amplitude patches exist in the scattered field, in agreement with concurrent theoretical developments.[8] These phenomena are also under intensive study by Russian investigators.[9]

We have re-established the long-path facility, and are currently completing modifications on the original system which will permit a much larger receiver bandwidth and very small apertures ($<<\rho_o$), in order to fully accommodate the spatial and temporal characteristics of the field. The system operates at 4880Å as before, but with 100 kHz chopping using a novel photoelastic modulator (Fig. 13), and a final (demodulated) bandwidth of 10 kHz. Photomultipliers are utilized to achieve a 100 dB SNR with the small receivers, and the original (dual) covariance receiver has been modified for high resolution at small separations. A new demodulator with the required bandwidth and linear phase response for undistorted transients has been designed with an 80 dB dynamic range.

The system parameters are summarized in Table VIII. The means utilized to achieve high resolution of the covariance are shown in Figure 14. The demodulator, shown in Figure 15, uses a Motorola Type 1496 balanced modulator with a Signetics 565 phase-locked-loop to supply the necessary constant-carrier input; the latter component functions properly over a very large dynamic range, so that severe fading will not interrupt the system. The required phase or transient response is obtained in a four-pole Bessel low-pass filter.

C. Further Plans

Following the efforts described above, the wander-tracking system will be modified to study the effects of enhanced "angular

---

8. H. T. Yura, J. Opt. Soc. Am. 64, 59-67, January 1974

9. M. E. Gracheva, et al, "Similarity Correlations and Their Experimental Verification in the Case of Strong Intensity Fluctuations of the Laser Radiation", preprint, August 1973.

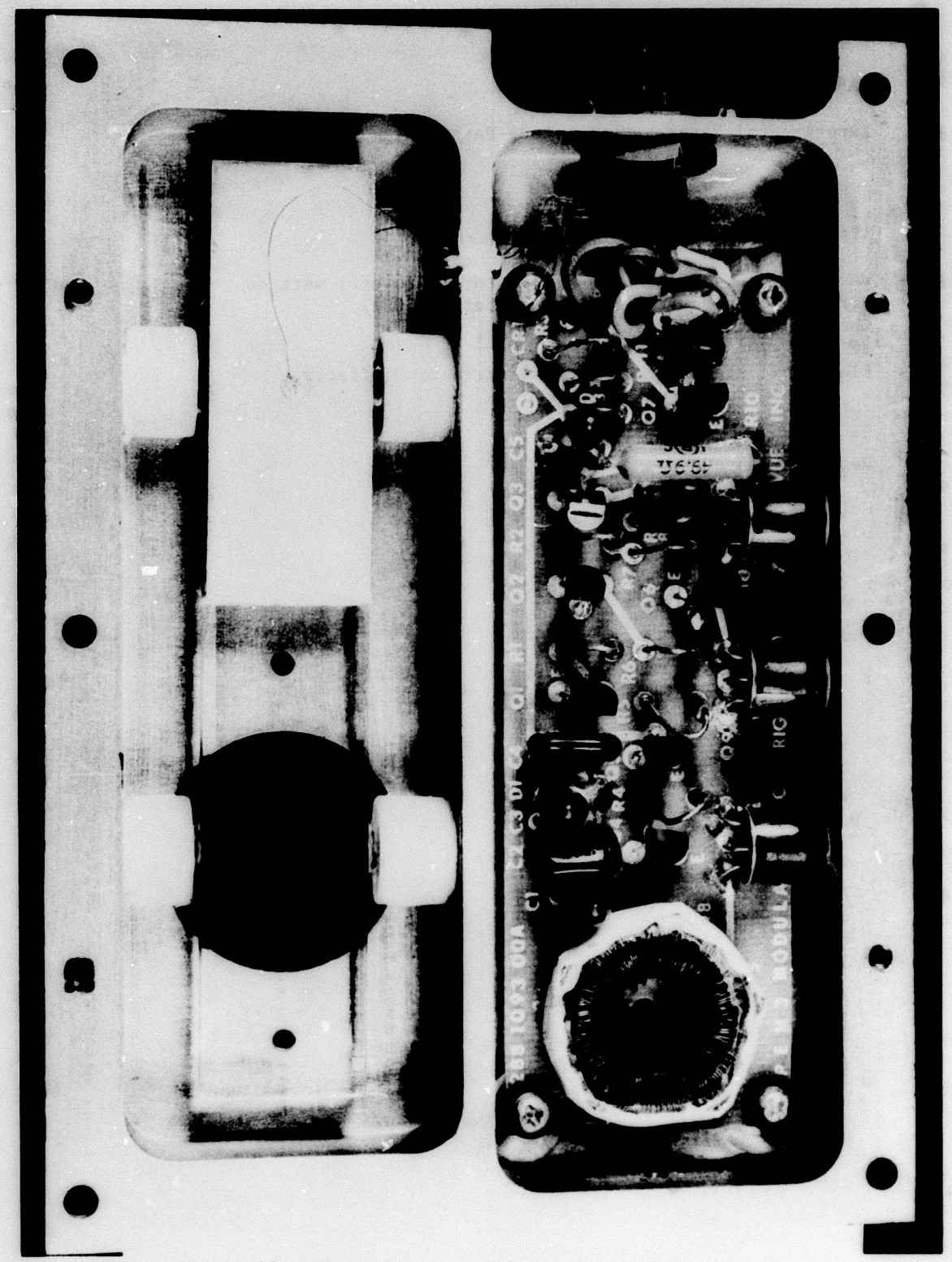

Figure 13. Photoelastic modulator for 100kHz chopping.

TABLE VIII

Experimental Parameters for Long-Path System

Transmitter Characteristics

Wavelength: 4880Å Power: 1 watt cw
Virtual-point-source (Fresnel number = 0.002)
Chopping rate: 100 kHz
Height: 7m
Electronic steering for diurnal refraction effects

Receiver Characteristics

Height: 4m
Diameter: 0.25mm-1mm
Minimum covariance separation: 0.25mm
Bandwidth: 10 kHz
Dynamic Range: > 80 dB
Processing:

Variance of log amplitude
Covariance
Statistics
Spectra

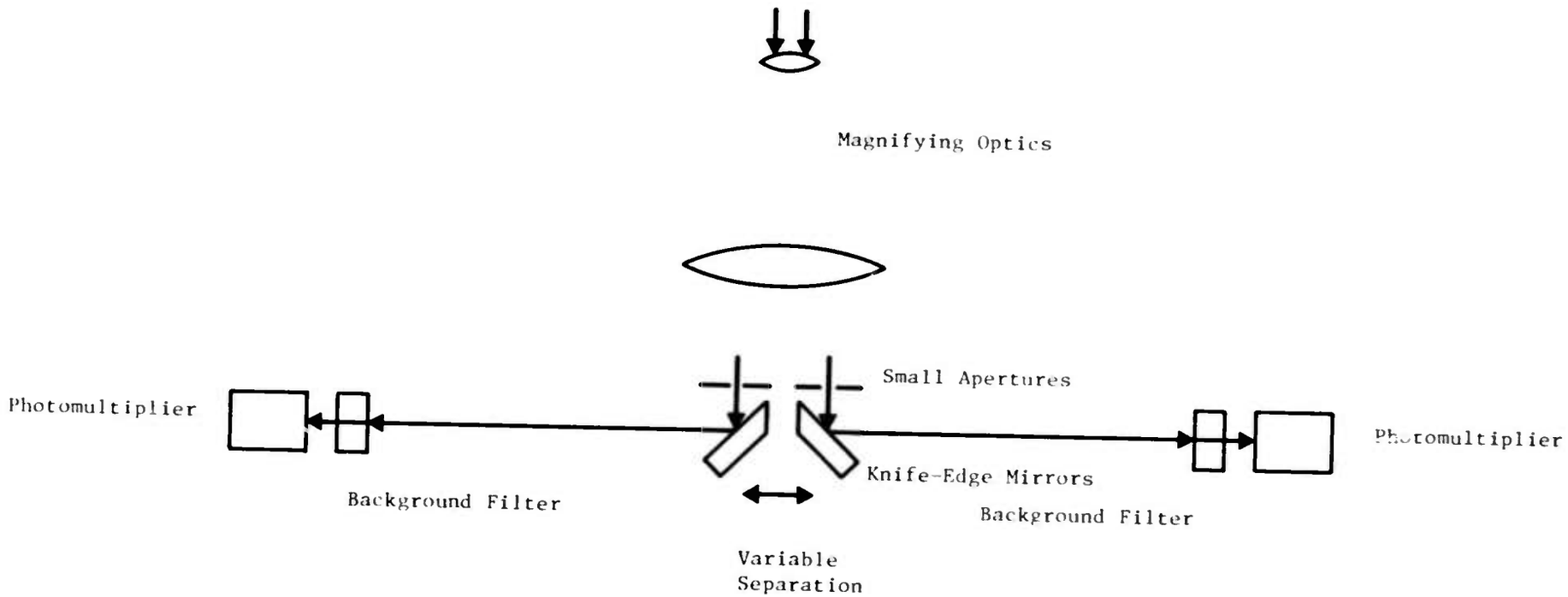

Figure 14. Diagram of high-resolution covariance receiver for long-path, strong-saturation measurements.

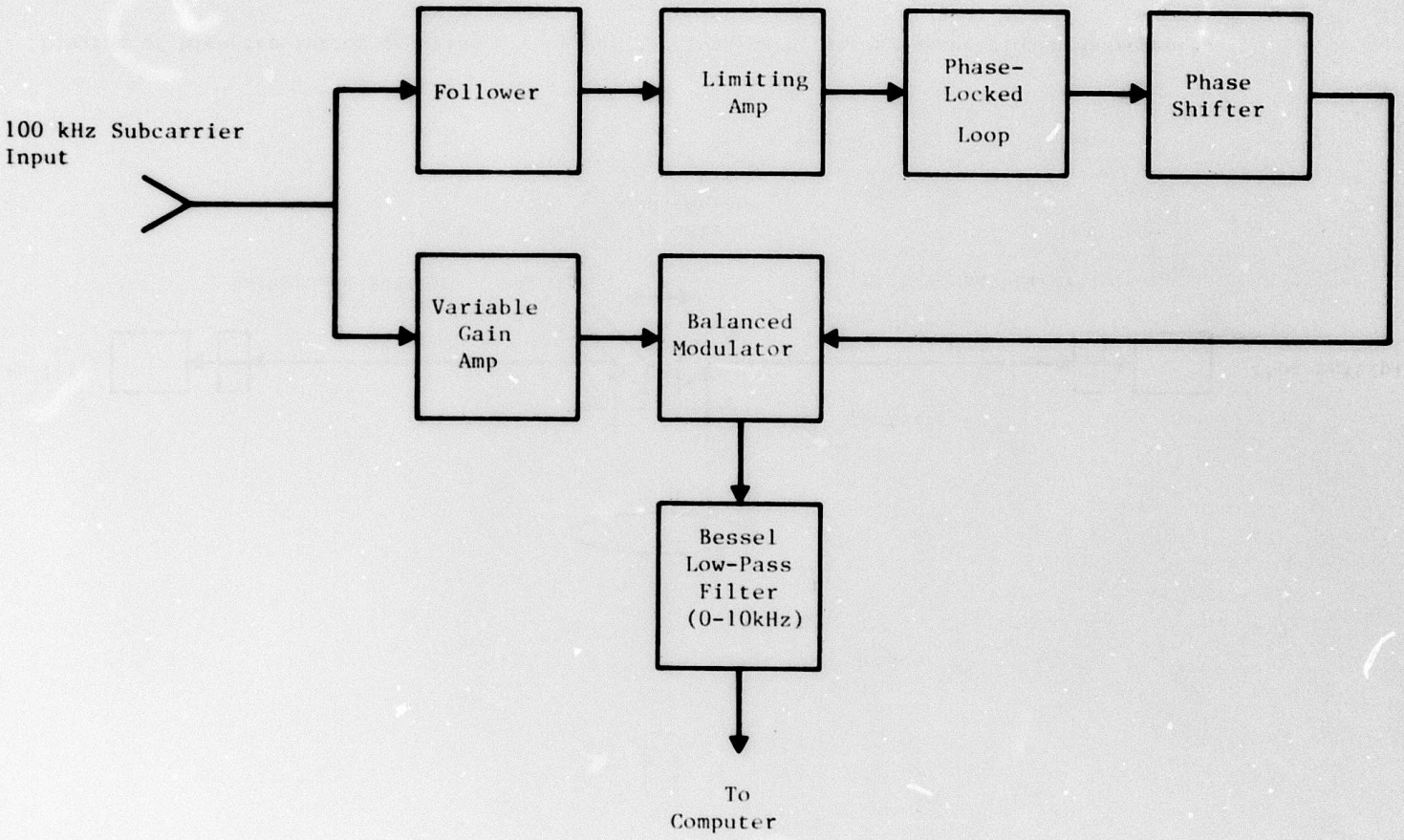

Figure 15. Diagram of wideband, large-dynamic-range demodulator.

scintillation" from a retroreflector.[10,11] Also, in a follow-on effort, the scintillation characteristics including covariance structure will be determined for extended, partially coherent (i.e., generalized) sources. This topic pertains to turbulence effects on "speckle" and has not been adequately understood; it pertains to such applications as remote sensing, and noise in adaptive transmitters.

---

10. J. P. Hansen and S. Madhu, Applied Optics 11, 233-238, February 1972.

11. R. F. Lutomirski, Applied Optics 14, 840-846, April 1975.

V. REFERENCES

1. J. R. Kerr, et al, "Propagation of Multiwavelength Laser Radiation Through Atmospheric Turbulence," RADC-TR-74-320, November 1974. (ADA003 340)
2. S. O. Rice, "Mathematical Analysis of Random Noise", in Selected Papers on Noise and Stochastic Processes, N. Wax., ed., Dover Publications, Inc., N. Y., 1954
3. J. W. Strohbehn, T. Wang, and J. P. Speck, Radio Science 10, 59-70, January 1975.
4. M. Abramowitz and I. Stegun, ed., Handbook of Mathematical Functions, Dover Publications, Inc., N. Y., 931-940, 1965.
5. J. R. Kerr and J. R. Dunphy, "Propagation of Multiwavelength Laser Radiation Through Atmospheric Turbulence", RADC-TR-74-183, May 1974. (AD783 277)
6. V. A. Banakh, et al, J. Opt. Soc. Am. 64, 516-518, April 1974.
7. J. R. Dunphy and J. R. Kerr, J. Opt. Soc. Am. 63, 981-986, August 1973.
8. H. T. Yura, J. Opt. Soc. Am. 64, 59-67, January 1974.
9. M. E. Gracheva, et al, "Similarity Correlations and Their Experimental Verification in the Case of Strong Intensity Fluctuations of the Laser Radiation", preprint, August 1973.
10. J. P. Hansen and S. Madhu, Applied Optics 11, 233-238, February 1972.
11. R. F. Lutomirski, Applied Optics 14, 840-846, April 1975.

MISSION
of
Rome Air Development Center

RADC is the principal AFSC organization charged with planning and executing the USAF exploratory and advanced development programs for information sciences, intelligence, command, control and communications technology, products and services oriented to the needs of the USAF. Primary RADC mission areas are communications, electromagnetic guidance and control, surveillance of ground and aerospace objects, intelligence data collection and handling, information system technology, and electronic reliability, maintainability and compatibility. RADC has mission responsibility as assigned by AFSC for demonstration and acquisition of selected subsystems and systems in the intelligence, mapping, charting, command, control and communications areas.